

JPRS 74138

6 September 1979

China Report

SCIENCE AND TECHNOLOGY

No. 7

Selections from 'QIXIANG', No. 4, 1978



FOREIGN BROADCAST INFORMATION SERVICE

NOTE

JPRS publications contain information primarily from foreign newspapers, periodicals and books, but also from news agency transmissions and broadcasts. Materials from foreign-language sources are translated; those from English-language sources are transcribed or reprinted, with the original phrasing and other characteristics retained.

Headlines, editorial reports, and material enclosed in brackets [] are supplied by JPRS. Processing indicators such as [Text] or [Excerpt] in the first line of each item, or following the last line of a brief, indicate how the original information was processed. Where no processing indicator is given, the information was summarized or extracted.

Unfamiliar names rendered phonetically or transliterated are enclosed in parentheses. Words or names preceded by a question mark and enclosed in parentheses were not clear in the original but have been supplied as appropriate in context. Other unattributed parenthetical notes within the body of an item originate with the source. Times within items are as given by source.

The contents of this publication in no way represent the policies, views or attitudes of the U.S. Government.

PROCUREMENT OF PUBLICATIONS

JPRS publications may be ordered from the National Technical Information Service, Springfield, Virginia 22161. In ordering, it is recommended that the JPRS number, title, date and author, if applicable, of publication be cited.

Current JPRS publications are announced in Government Reports Announcements issued semi-monthly by the National Technical Information Service, and are listed in the Monthly Catalog of U.S. Government Publications issued by the Superintendent of Documents, U.S. Government Printing Office, Washington, D.C. 20402.

Indexes to this report (by keyword, author, personal names, title and series) are available from Bell & Howell, Old Mansfield Road, Wooster, Ohio 44691.

Correspondence pertaining to matters other than procurement may be addressed to Joint Publications Research Service, 1000 North Glebe Road, Arlington, Virginia 22201.

REPORT DOCUMENTATION PAGE		1. REPORT NO. JPRS 74138	2.	3. Recipient's Accession No.
4. Title and Subtitle CHINA REPORT: SCIENCE AND TECHNOLOGY, No. 7 Selections from 'QIXIANG', No. 4, 1978				5. Report Date 6 September 1979
7. Author(s)				6.
8. Performing Organization Name and Address Joint Publications Research Service 1000 North Glebe Road Arlington, Virginia 22201				9. Performing Organization Rept. No.
10. Project/Task/Work Unit No.				11. Contract(s) or Grant(s) No.
				(C) (G)
12. Sponsoring Organization Name and Address As above				13. Type of Report & Period Covered
				14.
15. Supplementary Notes				
16. Abstract (Limit: 200 words) This serial report contains articles, abstracts and news items on national developments in science and technology; and physical, applied and life sciences in China.				
17. Document Analysis a. Descriptors CHINA National Developments Academia Sinica Physical Sciences Applied Sciences Life Sciences				
b. Identifiers/Open-Ended Terms				
c. COSATI Field/Group 01, 02, 04, 06, 07, 08, 09, 11, 12, 13, 20				
18. Availability Statement Unlimited Availability Sold by NTIS Springfield, Virginia 22161		19. Security Class (This Report) UNCLASSIFIED		21. No. of Pages 55
		20. Security Class (This Page) UNCLASSIFIED		22. Price

6 September 1979

CHINA REPORT
SCIENCE AND TECHNOLOGY

No. 7

SELECTIONS FROM 'QIXIANG', No. 4, 1978

CONTENTS	PAGE
Table of Contents of QIXIANG, Apr 78.....	1
Front, Back Cover Pictures.....	4
Developing County Meteorological Stations Urged.....	6
China Receives Data From Japanese Meteorological Satellite (Xiao Wenan; Jing Qiyi).....	11
Indices for Forecasting Continuous Rainy Weather (Yu Daren).....	14
Severe Thunderstorm Vertical Currents Studied (Wang Angsheng; Xu Naizhang).....	16
Influences of Air Temperature, Pressure on Aircraft Studied (Zhang Chaoguang).....	25
Tube-Type Telemetry Rain Gage Developed (Yuzhixin).....	29
Climatic Conditions Causing Wheat Scab Disease Outlined.....	37
Ditches Used to Prevent Moisture from Harming Three Wheats.....	48
Early Plum Rain Forecasting.....	51
Areas of Inclement Weather Conditions Reported.....	54

TABLE OF CONTENTS OF 'QIXIANG,' APR 78

Beijing QIXIANG [METEOROLOGY] in Chinese No 4, Apr 78 p 40

[Text] Table of Contents

*Energetically Develop County Weather Forecasting Stations Jiangxi Meteorological Bureau.....	1
Layman Becomes Professional—Story of Comrade Xin Jinhe [0207 6855 3109], Director of the Julu County Meteorological Station Xingtai Prefecture Meteorological Bureau, Hebei Province.....	2
Using Jet Axis and System Composite Charts to Forecast Precipitation Areas Huiyang Prefecture Meteorological Station, Guangdong Province...	3
Case Analysis of a Strong Typhoon Caused by a Descending High Altitude Cold Vortex Central Meteorological Station, Yang Zufang [2799 4371 5364]....	7
How to Analyze Satellite Cloud Photographs (VI) Analyzing Plateau Weather Cloud Pictures Li Yulan [2621 3768 5695].....	10
Ancient China's Knowledge of Physical Phenomena in the Atmosphere Zhang Deer [1728 1795 0059].....	13
Investigation and Preliminary Study of a Tornado Yang Qihua [2799 6386 5478], Chen Caitian [7115 2088 3944], Wu Muliang [0702 3092 5328].....	16
Experimental Use of Correlated Temperature and Pressure Data to Forecast Rainfall in May Zhao Hongsheng [6392 3163 5116].....	18

Discussion: "How to Properly Operate County Station Forecasting"

Stress Study of Basic Theoretical Knowledge Han Zhengfang [7281 2873 5364].....	20
County Station Forecasting Work Needs Big Leap Forward Song Xiangxin [1345 4161 0207].....	21
The Use of Lunar Calendar Terms in Weather Forecasting is Unscientific Zhu Congliang [2612 1783 0081].....	21
*Some Indices for Forecasting Long Continuous Cloudy and Rainy Weather in Spring Yu Daren [0060 6671 0086].....	25
*Japan's Geostationary Meteorological Satellites and China's Receiving Units Xiao Wenan [5135 4489 1344], Jing Qiyl [5427 0366 0001].....	22
*Probing Severe Thunderstorm Vertical Air Currents Wang Angsheng [3769 2491 3932], Xu Naizhang [1776 0035 3864]....	26
Estimating Mean Wind Speeds on Roof Tops of Tall Buildings Huang Houkang [7806 0624 1660].....	28
Lake and Land Breezes in Yueyang (Dongting Lakeshore) Li Lianfang [2621 6647 2455].....	30
*Influence of Air Temperature and Pressure on Aerial Flights Zhang Chaoguang [1728 2600 0342].....	31
Three Simple Tables for Ground Weather Observation Ceng Ling-gui [2582 0109 6311].....	9
A Small Improvement in Two-Way Telephones Used in High Altitude Wind Measurement System Chen Zhengcai [7115 2973 2088].....	15
*Research on Meteorological Instruments Tube-type Telemetry Rain Gage (Hyetometer).....	32
*Climatical Conditions Causing Wheat Scab Disease Operation Division, Shanghai Meteorological Bureau.....	35
Swapping Experiences Among Meteorological Posts *Proper Use of Ditches to Prevent Moist Calamities from Harming the Three Wheats Chonggu Middle School School Meteorological Post, Qingpu County, Shanghai.....	38

*Long Range Forecasting of Plum Rain Period Department of Geography, Red & Expert Normal School, Fengxian County, Shanghai.....	39
*Information.....	39
Why Are Temperature Data Signals from Radiosonde Equipments Unclear? Duan Caishi [3008 2088 1807].....	40
Answer to Problem in Last Issue: How to Use "Common Meteorological Table No. 1" Which Does Not Give Dew Point Information? Contributed by Li Yuan [2621 3293].....	40
*Front Cover, Outside: Make Contributions to Meteorological Research (Photographed by Jia Yujiang [6328 3768 3068])	
Front Cover, Inside: Geostationary Meteorological Satellite Cloud Photograph Receiving Unit Successfully Developed and Produced in China (Photographed by QIXIANG Magazine)	
Back Cover, Inside: Geostationary Meteorological Satellite Cloud Pictures	
Back Cover, Outside: Antenna of Receiving Unit for Picking Up Geo- stationary Meteorological Satellite Cloud Pictures	
*Translated and Published	

9119
CSO: 4008

FRONT, BACK COVER PICTURES

**Front Cover, Outside: Make contributions to meteorological research.
Photographed by Jia Yujiang [6328 3768 3068]**

Front Cover, Inside: Geostationary Meteorological Satellite (GMS) cloud photograph receiving unit successfully developed and produced in China

(1) In accordance with the great leader and teacher Chairman Mao's instruction: "the Chinese people have the will and ability to catch up with and overtake the world's advanced level in the not-too-distant future," and under the guidance of the wise leader Chairman Hua's strategic policy of taking firm hold of key links in running the country, the workers, cadres and technical personnel of the Atmospheric Physics Institute of the Chinese Academy of Sciences, the Nanjing Daqiao Machinery Plant, and the Shanghai Wired Radio Factory worked with revolutionary zeal and ardor, and succeeded in developing and producing a GMS cloud picture receiving unit before the scheduled launching of Japan's GMS satellite in July 1977.

The receiving unit picked up Japan's trial transmission of high resolution panoramic cloud pictures and low resolution zonal cloud pictures; the photographs were clear and of advanced-level quality. This achievement will contribute towards the further development of our country's meteorological forecasting operations and satellite meteorology.

(Photographed by QIXIANG)

(2) Researchers checking the quality of satellite cloud photo negatives. GMS cloud photo receiver antenna shown in upper right corner.

(3) Researchers analyzing resolution of GMS cloud picture negatives.

(4) Tao Shiyan, researcher of the Institute of Atmospheric Physics, Chinese Academy of Sciences, and other meteorological researchers studying GMS cloud photographs and analyzing the development of tropical atmospheric circulation in the Pacific Ocean Region.

Back Cover, Inside: Geostationary Meteorological Satellite cloud pictures.

(1) Top Picture: Japanese GMS high resolution cloud photo picked up by China's receiving unit.

(2) Bottom Picture: Japanese GMS low resolution zonal cloud photo picked up by China's receiving unit.

Back Cover, Outside: Antenna of receiving unit for picking up GMS cloud pictures.

9119

CSO: 4008

DEVELOPING COUNTY METEOROLOGICAL STATIONS URGED

Beijing QIXIANG [METEOROLOGY] in Chinese No 4, Apr 78 pp 1-2

[Article by Jiangxi Meteorological Bureau: "Energetically Develop County Weather Forecasting Stations"]

[Text] Guided by the beacon light of the three red banners--the general line, great leap forward and people's communes--in 1958, the broad ranks of our country's meteorological workers liberated their minds from superstition and blind faith, and vigorously developed county station weather forecasting work. The emergence of this new socialist phenomena manifests a tremendous force of vitality which has put an end to the old tradition of regarding meteorological stations merely as sites for providing meteorological information and collecting meteorological data. As a result, meteorological stations, which used to be purely grassroot operational units, have now been transformed into active combat units closely linked to the three revolutionary movements and play a vital role in providing party committees at all levels with useful information for organizing production, guiding production as well as preventing and combatting natural calamities. The emergence and development of county forecasting stations represent an important step by China's meteorological workers who are developing our country's meteorological work through independent and self-reliant efforts under the guidance of Chairman Mao's revolutionary line. The broad ranks of meteorological workers have been tempered through the Great Proletarian Cultural Revolution, especially in recent years through struggles to stamp out the disruptive activities of the "gang of four;" they have now further developed county forecasting stations, which is a new-born socialist phenomena. Through their efforts, the county stations are now playing a vital role in the three great revolutionary movements, especially agricultural production.

Through 6 years of continuous improvements, the county forecasting stations throughout our province have rapidly developed. Now, all the county meteorological stations have developed complete sets of basic charts and tables, basic materials and technical files on forecasting inclement weather which are unified for general use of the entire province.

Preliminary systems for producing inclement and critical weather forecasts have been developed. Through practice, we have formed an army of red and expert county station forecasting technicians. All this has greatly enhanced our ability to serve agricultural production.

In the course of reforming our county forecasting stations, we spent one year on experimentation, 2 years on popularization, and 3 years on foundation work. Through nearly 6 years of practical work in weather forecasting, the broad ranks of meteorological workers have acquired a better understanding of developing county forecasting stations, the broad ranks of meteorological workers have acquired a better understanding of developing county forecasting stations, both in terms of guidelines and specific tasks. The more they work, the more they want to do, and the more they work, the better they learn to work. Today, we are making improvements year after year, which has resulted in steady progress year by year. The following five main links are emphasized in our work:

The first link is foundation work, that is, the construction of county station operations. In 1971, in order to reform county station weather forecasting, we put forward a number of development proposals based on thorough investigation and study. First, it was necessary to develop a "composite factor time chart" as a basic tool for county station operations. The first year was focused on an experimental point, which was popularized in the second year. In the course of popularization, we picked out forecasting factors that had been proven relatively useful through several years of practical forecasting work, and from these factors, we eventually developed a unified basic data chart suitable for long, medium and short range forecasting. We also developed a unified system file for forecasting inclement weather. This was our preliminary achievement towards the completion of basic operational construction which consisted of basic charts, data and technical files required for our province's county weather forecasting stations.

The advantages of building a unified basis for county station forecasting operations are as follows: (1) Conducive to popularization and further improvements. In the past, there were many forecasting information charts which everyone was interested in, except that no one knew which one to study. The unification of charts and information not only provides convenience for users, but also makes it easier to learn and understand, and everyone has mastered the technique of plotting and analysis in a relatively short time. (2) Conducive to popularizing advanced experiences. In the past, owing to lack of data and chart unification, it was necessary to plot another set of charts and tables in order to study the advanced experiences of other stations, which entailed a great deal of excessive work, and the results were poor in terms of time efficiency. Today, things are different: modifications and substantiations are made only when necessary, which helps to improve the level of forecasting technique. (3) Conducive to discovering common laws governing weather development. After laying down the unified basis for operations, we found that there are common features in the

development of single-station factors on the same day in a given climatical activity area. The findings of one station are often of universal value throughout the entire area. By accumulating more and more experiences, it is possible to gradually deepen the understanding of the laws of weather development, and thus elevate perceptual knowledge to rational knowledge.

The second link is to focus on key problems, such as inclement weather which gravely affects agricultural production, and crucial weather conditions of major farming seasons. In the early stages of county station weather forecasting, the only operations involved were making additions to or correcting daily forecasting reports from large stations. There was lack of stress on key points or specific major targets, and, hence, it was impossible to solve major meteorological problems in agricultural production. With the in-depth development of the movement of "learn from Dazhai in agriculture," we began to realize that it was a mistake to limit county station forecasting operations to general weather forecasting and neglect inclement and crucial weather conditions. Thus, we came up with a specific proposal to have county stations center their forecasting work on the "three junctures," e.g. spring sowing, grain buds cold [1420 3341 1383] and cold dew wind [1383 7216 7364], the "three preventations," e.g. prevention against tides, prevention against drought, and prevention against insects. The county stations should concentrate their efforts on inclement weather relatively harmful to agricultural production, as well as crucial weather conditions of major farming seasons; they should provide accurate forecasts and information. Practice shows that specifying primary and secondary objectives and shortening the combat line helps to concentrate forces and produce quick results.

The third link is to conduct joint operations. As county stations are staffed with few people who have to handle many tasks, we do not think it is feasible for county stations to carry out forecast reformation projects independently of each other. In accordance with Chairman Mao's instructions "concentrate superior forces to wipe out the enemy," since 1972, we have organized joint provincial forecasting operations through the provincial bureau; the operations include searching for methods, training basic working forces, and accumulating experiences. Beginning in 1974, we combined the efforts of all forces under a centralized provincial plan with unified requirements using regions as units; the joint operations were carried out in concentrated periods of time, lasting 2-3 months each year. Emphasis was laid on attacking inclement weather and critical weather, and the general process was to tackle each problem one by one. Through 6 years of joint operations, the stations throughout our province developed a relatively useful universal system for making medium and short range forecasts during spring sowing and tidal periods, which proved to be quite successful in actual service. We also managed to fill in some of the blank areas, which has greatly promoted the growth of county station weather forecasting.

The fourth link is to develop combined preventive operations. There are many hilly and mountainous areas in our province. Owing to topographical influences, plus complicated weather conditions, it is difficult for large stations and single stations to discover fast moving and devastating medium and small scale inclement weather which frequently hit the area. In 1971, some stations got organized during tidal periods and carried out concerted operations to protect water reservoirs in their respective areas, and the combined efforts to protect key points turned out to be quite successful. We promptly summarized and popularized this experience, and further developed the coordination between stations to jointly prevent all sorts of inclement weather disasters that occur in farming seasons. Now, besides joint preventive operations of county stations and their subunits, most of the stations throughout the province have organized joint protection areas, and, in some cases, joint operations with stations in neighboring provinces have been carried out. Through several years of practice, we have come to realize that joint prevention is conducive to monitoring the development of inclement weather. With frequent station observations, it is possible to discover the development of meteorological factors at any given time, and thus reflect the occurrence, development and movements of weather systems. This provides weather outposts with timely information and a basis for forecasting. Moreover, through mutual reinforcement and mutual promotion, it is possible to improve inclement weather monitoring capability and forecasting accuracy rate equivalent to those of radar, even without use of actual radar systems. Joint preventive operations also help to solve the problems of precipitation gauges for forecasting work, thus enabling stations in the lower reaches of the weather system to produce specific reports which provide sufficient basis for making relatively accurate qualitative and quantitative forecasts, and sometimes even to the extent of predicting the exact time when precipitation starts and ends. Joint preventive operations make it possible to capture medium and small scale weather systems which are not found in weather charts, thus enabling meteorologists to quickly identify and accurately determine all sorts of medium and small weather systems brought about by local thermal and dynamic conditions. The operations also enable meteorologists to find out about variations in medium and small weather systems.

The fifth link is management. In the past, the county stations in our province used to manage observation and forecasting at the same time, which often makes it very difficult to manage county station forecasting operations. This was a lesson to us, and subsequently we implemented a coordinate system of dividing work among stations from provincial level down to regional level, thus ensuring the organization of various levels. We also specified the requirements of managing county station forecasting work, and put special emphasis on the guideline of serving agricultural production by attacking inclement weather, relying on the masses in weather management, promoting coordination among stations and outposts, adhering to rational codes and conventions, making serious efforts in quality inspection and comparative evaluation, and commending advanced units. The management of weather stations should pay attention to county units, conduct in-depth investigation and study routines, promote work in all areas by concentrating

on selected basic units, develop model units, mobilize all active elements, reform county station forecasting work, and make sure that county station forecasting work will always develop healthily along the correct line.

Looking in retrospect on the glorious years of the past, and looking ahead into the future with even higher spirits, we are determined to smash the "gang of four," develop the excellent situation, improve the technical level of county stations, and make greater contributions to the realization of the Four Modernizations under the leadership of the Party Central Committee led by the brilliant leader Chairman Hua.

9119

CSO: 4008

CHINA RECEIVES DATA FROM JAPANESE METEOROLOGICAL SATELLITE

Beijing QIXIANG [METEOROLOGY] in Chinese No 4, Apr 78 pp 22-25

[Article by Xiao Wenan [5135 4489 1344] and Jing Qiyi [5427 0366 0001]: "Japan's Geostationary Meteorological Satellites and China's Receiving Units"]

[Excerpts] On 14 July 1977, Japan successfully launched a Geostationary Meteorological Satellite (GMS). The satellite was launched in accordance with the requirements of a global atmosphere research project. The World Meteorological Organization (WMO) plans to launch five GMS satellites in the 1970s, which will form a global atmosphere observation network together with two Polar Orbiting Satellites (POS) already in operational mode (Figure 1). So far, four satellites have been put into orbit: two Synchronous Meteorological Satellites (SMS-1 and SMS-2); one Geostationary Operational Environment Satellite (GOES-1); and one Geostationary Meteorological Satellite (GMS). The first three satellites were launched by the United States in May 1974, February 1975 and December 1975. SMS-2 and GOES-1 are the two operational satellites currently in working mode, and SMS-1 is a standby satellite. The other two satellites are to be launched by Europe and the Soviet Union, but so far their projects have not been completed yet.

Our country is situated within the observation range of Japan's GMS satellite. Following is a brief introduction to the GMS and China's receiving unit. [Paragraphs on the function, structure and ground station of the Japanese satellite omitted]

II. China's Receiving Unit

GMS observation data plays a very important role in weather analysis and forecasting in areas within the observation range. The observation range of the satellite extends from 80 degrees east to 160 degrees west, from 50 degrees north to 50 degrees south, which thus includes the Pacific Ocean, the eastern part of the Indian Ocean, the eastern part of the Asian continent, and Oceania. The satellite can continuously monitor the occurrence,

development and weakening of major weather systems in typhoon and tropical convergence regions. Based on the movement of tropical cloud fields, it is possible to deduce the tropical flow field, and therefore study and analyze the laws governing the development of tropical atmospheric circulations; such cloud pictures can also be used for studying the interaction between atmospheric circulations of the northern and southern hemispheres. Besides, as the GMS satellite can make continuous observations, it provides a very useful means of tracking and studying medium and small scale weather systems.

In early 1977, a concerned research unit in our country began to develop receiving units for picking up GMS signals. In July 1977 (before the GMS was launched), the development project was completed. In mid August 1977, we picked up adjustment signals from the GMS; high and low resolution facsimile test cards were also received. Now, we have already started to receive GMS trial transmissions of high resolution cloud pictures as well as low resolution zonal cloud pictures (see inside page of back cover).

China's receiving unit for picking up GMS transmission consists of a 6-meter diameter circular parabolic antenna, a WT-1 cloud picture main receiver, a 121 cloud picture facsimile apparatus, and a 118 facsimile apparatus. (See block diagram of receiving unit in Figure 7)

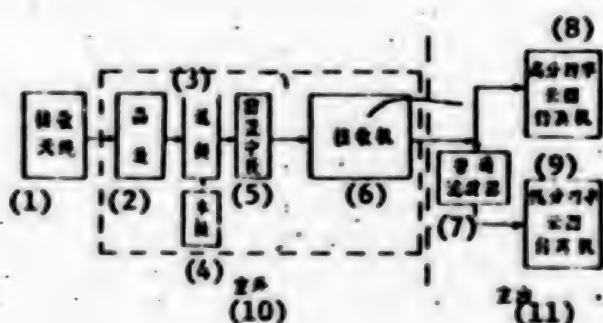


Figure 7 Block diagram of GMS facsimile cloud picture receiver

- | | |
|------------------------------|---|
| (1) receiving antenna | (7) band filter |
| (2) transistorized amplifier | (8) high resolution cloud facsimile apparatus |
| (3) frequency mixer | (9) low resolution cloud facsimile apparatus |
| (4) local oscillator | (10) outdoor portion |
| (5) IF prime amplifier | (11) indoor portion |
| (6) receiver | |

The antenna is a modified 6-meter diameter circular parabolic antenna. The main components of a WT-1 satellite cloud high-frequency (HF) receiving unit are installed inside a cylindrical case. A symmetric semi-wave vibrator is mounted at the end of the case. The entire HF equipment cylinder is placed at the focal point of the paraboloid. The characteristics of the antenna and HF unit are shown in Table 2.

The receiver is a modified version of the WT-1 main receiver. A band filter is added to the unit in order to pick up high resolution and low resolution facsimile loud photos. The main characteristics of WT-1 are listed in Table 3.

In the facsimile system, the channel transducer circuit of a 121 cloud facsimile apparatus is closed off and supplemented with a 118 cloud facsimile unit.

Table 2 Main Characteristics of Antenna and HF Unit

Item	Parameter
antenna diameter	6 m
focal distance	2.3 m
frequency	1690 MC \pm 10 MC
antenna beam width	2 degrees
gain	38 db
HF amplifier noise factor	4 db
HF amplifier gain	25 db
1st IF frequency	137.5 MC

Table 3 Main Characteristics of WT-1 Main Receiver

Item	Parameters
input frequency	137.5 MC
receiver band width	A 1 MC B 300 KC
output signal	A 9 KC \pm 29 KCPH B 2.4 KCAM

9119
CSO: 4008

INDICES FOR FORECASTING CONTINUOUS RAINY WEATHER

Beijing QIXIANG [METEOROLOGY] in Chinese No 4, Apr 78 p 25

[Article by Yu Daren [0060 6671 0086]: "Some Indices for Forecasting Long Continuous Cloudy and Rainy Weather in Spring"]

[Text] Based on surveys, within the period of 21 years from 1957 to 1977, the three wheats [barley, wheat and naked barley] of Yangzhou Prefecture were hit by three grave waterlogging calamities in 1963, 1964 and 1977. All three calamities occurred in the months of April and May with over 20 days of continuous rain and clouds. The total rainfall exceeds 150 mm, and the number of rain days in that period accounted for more than 75 percent of the total duration of rainy and cloudy days.

Owing to the fact that the three wheats were not damaged by the water at the very outset of the cloudy and rainy period, such preventive measures as digging water drainage ditches, lowering the level of subterranean water, etc., could be taken if the long and continuous cloudy and rainy weather could be accurately forecast. This would not only safeguard the three wheats against waterlogging, but also ensure bumper harvests. With this object in mind, we made special analysis of the development of pressure, temperature and humidity curves recorded at this station prior to the three long continuous rainy and cloudy events, and obtained the following indices for forecasting long continuous cloudy and rainy weather in spring:

Table: Indices for forecasting long and continuous cloudy and rainy weather in spring

(1) 年 份	(2) T ₁₄ 逐日上升			(3) e ₁₄ 逐日增加		
	(4) 期 (月·日)	(5) 天 (天)	(6) ΣΔT ₁₄ (°C)	(7) 期 (月·日)	(8) 天 (天)	(9) ΣΔe ₁₄ (mb)
1963	4.6-14	8	21.0	4.10-14	4	13.3
1964	3.23-31	8	20.4	3.27-31	4	10.6
1977	4.7-23	8	15.2	4.10-23	5	21.3
(9) 1.	3.1月	≥8	≥15.0 T ₁₄ ≥ 15.0		≥4	≥10.0

- (1) year
- (2) T₁₄ daily increase
- (3) e₁₄ continuous increase
- (4) period (month . day)
- (5) number of days (days)
- (6) period (month . day)
- (7) number of days (days)
- (8) mb
- (9) indices

年	(2) 连续下降			(3) 连续阴雨				
(1) 年	(4) (月.日)	(5) (天)	(6) (mm)	(7) (月.日)	(8) (天)	(9) (%)	(10) (mm)	(11) (mm)
1963	4.7-11	7	22.3	4.17-5.15	30	28	258.4	
1964	3.22-31	6	21.9	4.1-5.1	31	82	211.9	
1977	4.18-23	6	14.3	4.22-5.20	22	81	157.7	
(11) 年	.	≥5	>12.0	4-5月	≥20	>75	>150.0	

- (1) year
- (2) P₁₄ continuous precipitation
- (3) long continuous cloud and rain
- (4) period (month.day)
- (5) number of days
- (6) mb
- (7) period (month.day)
- (8) total number of days
- (9) rain day percentage (%)
- (10) total rainfall (mm)
- (11) indices

With the above forecasting indices, it is possible for our area to determine within 3 days the beginning and duration of the long continuous spring rain period by combining it with related weather conditions (e.g. cold front, shifting of rain area). Through reexamination of historical data extending over 21 years, we have found that whenever the indices were reached in March and April, there were no instances where long continuous cloudy and rainy weather failed to occur. Moreover, long continuous rainy and cloudy weather never occurred when the indices were not reached. What merits our attention is the fact that when the indices are almost reached, it is possible that continuous cloudy and rainy weather will occur; the duration and magnitude of rainfall is determined by combining with other factors.

9119

CS0: 4008

SEVERE THUNDERSTORM VERTICAL CURRENTS STUDIED

Beijing QIXIANG [METEOROLOGY] in Chinese No 4, Apr 78 pp 26-29

[Article by Wang Angsheng [3769 2491 3932] and Xu Naizhang [1776 0035 3864]:
"Probing Severe Thunderstorm Vertical Air Currents"]

[Text] Severe thunderstorms have attracted the most attention in research on vertical air currents. Severe thunderstorms are the source of such major inclement weather as rainstorms, hail, thunder and lightning, strong thunderstorm winds, and tornados. The birth, growth and dissipation stages of the phenomena are closely related to the vertical currents within the clouds.

Besides using the common method of probing into vertical air currents with all kinds of balloons, in recent years more and more meteorologists are probing into vertical currents outside the strong thunderstorm clouds with Doppler radar, airplanes, radar tracking tracers, dropsondes, and all sorts of combined remote sounding methods.

The Doppler radar is an important piece of equipment which utilizes the Doppler Effect caused by cloud particle motion to probe cloud currents. When the electromagnetic wave source and the target are in relative motion, a frequency shift takes place in electromagnetic waves returning from the object to the wave source, thus producing the so-called Doppler Effect. The relations between frequency change Δf , wavelength λ , and velocity of motion V are expressed as follows:

$$\Delta f = \pm \frac{2V}{\lambda}$$

With cloud particles as targets, the meteorological Doppler radar enables us to study the field structure of cloud air currents. Figure 1 is a storm current structure diagram recently obtained through dual Doppler radar conjugated observations by foreign scientists. It only shows a two dimensional air current structure on an X - Y plane located in a 6.4 kilometer high stratum ($Z = 6.4$ km). The current structures of all horizontal strata can also be done likewise. It is moreover possible to produce vertical current data on X - Z and Y - Z planes. From the diagram, it can be readily

seen that on the X - Y plane, there is an anticyclonic circulation center at $x = 8$ km, $y = 15$ km; and a cyclonic circulation center at $x = 4$ km by $y = 5$ km. Observation of the entire storm indicates that the severe thunderstorm has a strong updraft on the vertical plane in the vicinity of $y = 11$ km and the area of $x = 8-12$ km. Through combined dual Doppler radar observation, we can obtain the three-dimensional structure of the storm current and information on its development history, which is extremely valuable.

Dropsondes provide flexible means of observing vertical current fields inside and outside the clouds although they are somewhat limited by thunderstorm weather. Thus, in recent years, armoured aircraft have been employed to observe vertical currents and other parameters in thunderstorms; dropsondes and telemetry instruments ejected from rockets have also been used to measure the vertical movements within clouds in hazardous areas. These methods have produced preliminary information.



Figure 1 Diagram showing part of a storm current structure as observed through dual Doppler radar (sketch of X-Y plane current, $Z = 6.4$ km)

Another method that is quite extensively employed is the use of tracers ejected from airplanes (or other means). Ground radar keeps track of the tracers which enable the measurement of vertical currents. Tracers are masses of very fine metallic foils or thin nylon threads coated with metallic substance. The tracers fall very slowly through the air. As their final velocity is so small and can be thus neglected as compared with the strong vertical air motion, the tracers can represent the air motion. However, this method cannot be used in severe thunderstorm cloud areas because the tracers are superceded by the reflectivity of echo waves, and the radar cannot keep track of them.

For many years, all kinds of methods have been used by countries around the world to probe severe thunderstorm vertical currents, and common results have been achieved through such extensive surveys. It is widely believed that strong vertical current fields form the structural framework of severe thunderstorms, and that their occurrence and termination directly affect the existence and disappearance of the cloud cells. The cloud cells of

strong thunderstorms are composed of two interacting vertical current systems which are organized and continuous, and are not characterized by instantaneous pulsation. Thus, the systems can continuously affect the cloud cells over a period of time. Figure 2 is a simple diagram of a thunderstorm model which shows two organized circulations: One is an up-lifting circulation moving in the direction of the cloud drift and composed of a current rising slowly into the clouds from below; the other is a descending circulation on the left side of the cloud, which is related to the precipitation. The two circulations form the framework of the cloud cell. The updraft, in particular, plays the dominant role in the formation and development of the cloud cell as it pulls the cloud anvil in the direction of the upper wind in the high altitudes while another portion turns into downward motion. Figure 3 shows the altitudinal development of an organized updraft, which, for the first time, we managed to observe by planting a multi-circuit remote sounding system inside an ascending thunderstorm cloud current at 23:26 on 10 August 1965. As we can see in the diagram, the updraft rapidly increases with the altitude. At 6 km altitude, the vertical current reaches the maximum rate of 12.9 m/sec; subsequently, it starts to decline; and after it exits from the cloud, it is compensated by a weak downdraft. To a certain degree, this type of updraft distribution is typical, and indicates that the uplifting current is organized. There is always a downdraft corresponding to the updraft; it appears when the cloud cell reaches the mature stage, and it is related to precipitation.



Figure 2 Schematic model diagram of thunderstorm cloud current structure

- | | |
|-------------------------------------|--------------------|
| (1) direction of thunderstorm drift | (7) inflow |
| (2) cloud anvil | (8) updraft |
| (3) radar forward hanging echo | (9) squall front |
| (4) weak echo wave area | (10) precipitation |
| (5) new cloud turret | (11) outflow |
| (6) cloud base | (12) downdraft |



Figure 3 Probe data of an organized thunderstorm updraft

- | |
|------------------------------|
| (1) altitude (km) |
| (2) exit cloud |
| (3) enter cloud |
| (4) vertical current (m/sec) |

The organized vertical current data as shown in Figure 4 was obtained from a descending current at 14:49 on 23 July 1964. It can be seen from the diagram that as the sounding balloon reached almost 2.5 kilometers and entered the descending current area of a cloud cell, it began to accelerate downwards at the initial velocity of nearly 5 m/sec. By the time it reached the altitude of approximately 1 km, its velocity increased to the maximum value of approximately 14 m/sec; and when it neared the ground surface, its speed decreased. Generally, updrafts are closely related to the birth and sustenance of cloud cells as they bring continuous and massive supplies of water vapor which are needed for cloud cell formation as well as for supporting the growth of cloud particles. On the other hand, downdrafts are often related to the decay and dissipation of cloud cells, and sometimes the cloud cells collapse under the direct impact of heavy precipitation. However, the expanding cold wet air current of the downdraft approaching the ground surface also helps to lift the warm wet current flowing into the front portion of the thunderstorm, which is conducive to the development or maintenance of new-born cloud cells. Besides organized ascending and descending air circulations, there are also relatively weak vertical currents in other parts of the cloud cells. Thus, the two circulations are generally considered as the basic framework of thunderstorms. Of course, the vertical currents in the ever-changing thunderstorm clouds also undergo changes in the various stages and positions. But such basic features are common characteristics.

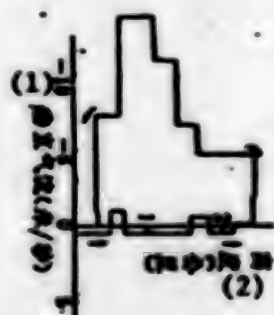


Figure 4 Probe data of an organized thunderstorm downdraft

- (1) altitude (km)
- (2) vertical current (m/sec)

As the birth and growth of thunderstorms are closely linked to the vertical updraft, a lot of effort has been devoted to the research on uplifting currents. Table 1 gives some information on certain parts of our country; it includes the maximum values of updrafts in several thunderclouds and hailclouds. Our country has managed to detect updrafts up to 15 m/sec which occurred approximately in the intermediate area of cloud layers. Statistics of the preceding parameters reveal that the maximum vertical currents (W_{max}) averages 10.8 m/sec, the departure being 2.7 m/sec; its altitude above the cloud base is 2.9 km, and the departure is 1.0 km; the mean cloud breadth is approximately 6.1 km, and the departure amounts to 1.3 km.

Table 1. Some information on thunderstorm vertical updrafts observed in certain parts of our country

(1) 号	(2) 云 种	(3) 时 间	(4) 地 点	(5) 最大垂直上升速度 (m/sec)	(6) 云底以上高度 (km)	(7) 云宽 (km)	(8) 方 法
1	雷暴云	1961.7.26 12:45	南京	10.2	2.1	0.6	仪器
2	雷暴云	1961.7.13 17:36	北京	6.9	2.6	4.0	仪器
3	雷暴云	1961.8.10 23:00	北京	12.9	6.0	0.5	仪器
4	雷暴云	1970.8.3 15:20	青海省民和县	12.2	2.5	4.5	计算
5	雷暴云	1972.7.5 16:30	甘肃省岷县	14.1	1.6	6.7	计算
6	雷暴云	1972.7.20 14:17	甘肃省岷县	6.9	2.0	2.0	计算
7	雷暴云	1972.7.25 13:20	甘肃省永登县	12.3	2.6	6.0	计算

- | | |
|------------------------------|--------------------------------------|
| (1) Number | (5) Maximum Vertical Current (m/sec) |
| (2) Cloud Cell | (6) Altitude Above Cloud Base (km) |
| a. thundercloud | (7) Cloud Breadth (km) |
| b. thundercloud | (8) Method |
| c. thundercloud | a, b, c instrument |
| d. hailcloud | d, e, f, g calculation |
| e. hailcloud | |
| f. hailcloud | |
| g. hailcloud | |
| (3) Time of Balloon Sounding | |
| (4) Place | |
| a. Nanjing | |
| b. Beijing | |
| c. Beijing | |
| d. Huzhu County, Qinghai | |
| e. Min County, Gansu | |
| f. Min County, Gansu | |
| g. Yongdeng County, Gansu | |

For comparative study of conditions in China and foreign countries, we have tabulated the identical results of observations made in the Soviet Union and the United States in Table 2. It is not difficult to see that the data from these countries are quite close. Apparently, if the size of the cumulus cloud is small, the maximum vertical current is also small. In all three countries, the 46 pieces of information ranging from the thickest cumulus clouds to hail clouds reveal that the maximum vertical currents are 10.8-17.4 m/sec, which are stronger than ordinary cumulus clouds; the departure values range from 2.7 m/sec to 4.2 m/sec; the arithmetical mean values are $\bar{x} = 13.9$ m/sec, $\bar{s} = 3.4$ m/sec. The altitude of the corresponding maximum current above the cloud base is 1.6-2.9 km, and averages 2.3 km; the departure is 0.6-1.0 m/sec; the mean rate is 0.8 m/sec. On the whole, the maximum cloud cell vertical currents are basically distributed in the lower central portion of the strong convection cloud cells.

Table 2 Some information on convection cloud vertical updrafts observed in several countries

(1) 序号	(2) 国家	(3) 云 型	(4) 数 量	(5) 最大垂直速度 平均/公里	(6) 最大上升速度 平均/公里	(7) 观测方法
1	中国	雷暴云和积雨云	7	10.4/2.7	2.9/1.0	气球携带仪器观测
2	美国科罗拉多州	积雨云	15	17.1/1.2	2.5/0.9	雷达跟踪追踪
3	苏联	有降水层的积雨云	7	12.1/2.2	1.5/0.6	气球携带仪器
4	苏联	无降水层的积雨云和积雨云	17	14.1/2.4	2.1/0.7	气球携带仪器
5	苏联	积雨云和积雨云	22	7.4/1.7	1.0/0.1	气球携带仪器
(8) 强对流云—中强对流云平均(算术)			46	13.9/2.1	2.3/0.8	各种方法 (9)

- (1) Number
 (2) Country
 a. China
 b. Colorado, U.S.A.
 c. USSR
 d. USSR
 e. USSR
 (3) Cloud Type
 a. thundercloud & hailcloud
 b. hailcloud
 c. precipitating cumulus
 d. non-precipitation thick cumulus and cumulonimbus
 e. cumulus and cumulus mediocris
 (4) Frequency
 (5) Maximum Vertical Mean Value/Deviation
 (6) Altitude Above Cloud Base, Mean Value/Deviation
 (7) Observation Method
 a. balloon-carried instruments or calculation
 b. radar tracking tracer
 c. balloon equilibrium method
 d. balloon equilibrium method
 e. balloon equilibrium method
 (8) Strong convective clouds (arith.) average in all countries (1-4)
 (9) All kinds of methods

From the development of vertical currents through time and space as observed in the different countries, we can find the following characteristics:

Throughout the formation, growth and dissipation of a severe thunderstorm, the updraft plays an important part. It undergoes sharp changes in time and space, and also undergoes the process of growing from weak to strong, continued full force, and from decay to total dissipation. Figure 5 shows the results of continuous observations of a cloud cell. As shown in the diagram, from 16:37 to 17:20 the cloud vertical current gradually grew from strong to weak; the variation of its maximum vertical current was relatively sharp, and the cloud cell continued to deteriorate until total

disappearance. Through numerous observations, we have come to realize that although strong updrafts undergo tremendous changes as shown in Figure 5, and even though vertical currents can vary as much as double or triple the original values, the altitudinal changes of the maximum vertical current in a given period of time is not so great, which reflects the dynamic feature of supporting vertical currents: i.e. although the intensity may change, there is little variation in the optimum space conditions when the maximum value is reached. As strong updrafts help to form weak echo areas in clouds, meteorologists generally obtain valuable information through observations on the weak areas of cloud cells.



Figure 5 Strong cloud uplifting current developing through space and time.

- (1) altitude (km)
- (2) time when tracer was ejected
- (3) cloud base
- (4) vertical current (m/sec)

As shown in Figure 2, the horizontal inflow entering the cloud gradually inclines into a vertical current; with the help of the X-Z (or Y-Z) cross section, we can obtain the slopes of the updraft at all moments. Figure 6 represents the results of an observation conducted in a foreign country on 15 July 1971: From 15:42 to 17:00, the angle of inclination between the draft axis and the vertical direction (α) changed from 30 degrees to 10-15 degrees, which indicated that the vertical current was entering the clouds at a steep angle. Extensive observations showed that the inclination angle α was related to the factors behind the formation of vertical circulations. Usually, when the convection is warm, the inclination angle becomes relatively small and the thunderstorm drifts at a relatively slow speed. The inclination angle is also relatively small when the formation of the thunderstorm is accelerated by steep mountain relief. In the case of thunderstorms caused by frontal surfaces, squall lines and other dynamic factors, owing to the strong horizontal convergence, the inclination angle often becomes relatively large and steady. Generally, α often ranges from 30 to 60 degrees. If the strong thunderstorm is relatively continuous and stable, so is the value of α .



Figure 6 Locus diagram showing slopes of inflowing tracers on 15 July 1971

- (1) altitude (km)
- (2) horizontal path distance (km)

Squall front—i.e. the border between the inflow of strong thunderstorm updraft and the surface outflow of precipitation downdraft. (See Figure 2) To a certain extent, its position also reflects the dynamic features of cloud cells. The movements of the strong downdraft and the cloud precipitators are related to their dynamic backgrounds, and increasingly stronger cloud cells often cause the downdraft motion to become increasingly stronger; as the downdraft diverges at the ground surface, it is bound to interact with the updraft. The strong descending current often causes the squall front to expand forwards. People on the ground surface often determine squall fronts by observing the sharp wind changes before and after the squall fronts; some people have also used the distance between the squall front and ground surface at the front edge of the major rainfall area as a means of determining the approximate intensity of thunderstorms.

Owing to the importance of strong thunderstorm vertical movements, the results of research efforts in this area have already been extensively applied in cloud physics and the artificial ways of modifying local weather. In the early 1960s, preliminary results were achieved in the parabolic vertical distribution of convective vertical currents, which led people to believe that the top and middle portions of cloud updrafts could "accumulate" water. Through radar observations, it was discovered that the intensive portion of the hail cloud cell's "forward hanging echo" area was related to the strong updraft support, and that it could supply the "water-content accumulation zone" of the rapidly growing hail, which was a preliminary revelation of the physical picture of the rapid growth of hail. It was on this basis that the principle of preventing hail by "over-seeding" the water-content accumulation zone was found. This principle has not only made it possible to reduce the difficult process of introducing crystal catalysis into giant cloud cells down to 1/1000 of its size in the accumulation zone, but also enabled us to make the physical picture of the artificial modification model.

The vertical current has tremendous impact on the birth and dissipation of cloud cells. It also helps us to study ways of modifying the air currents of natural cloud cells through dynamic influence as well as various ways of changing precipitation or preventing hail. The working people of our country have extensively used explosives to modify precipitation and prevent hail, using the updrafts as the primary targets. It is conceivable that at a given time and position, a sufficient amount of explosion can affect clouds and precipitation. Explosions can affect the cloud updrafts by rapidly changing the equilibrium (quasi-stable or unstable) status of particles in the currents, thus causing them to precipitate. The precipitating particles can bring about downdrafts which accelerates the precipitation and dissipation of cloud cells. Moreover, the final velocity of massive fragments produced by the violent explosions can contribute partly to the downdraft movement which accelerates the dissipation of cloud cells. It is precisely due to such important factors of vertical currents that people have been probing deeper into the principles of explosion impacts.

The artificial updraft modification technique is also used for artificial downdrafts. By weakening or "stamping out" the uplifting movements, it is possible to exert artificial modification. In sum, more and more attention is being devoted to the research on severe storms. The research on and application of the major characteristics of storm currents are greatly emphasized, and it is anticipated that the research on severe thunderstorm vertical currents will play a vital role in weather forecasting and artificial weather modification.

9119

CSO: 4008

INFLUENCES OF AIR TEMPERATURE, PRESSURE ON AIRCRAFT STUDIED

Beijing QIXIANG [METEOROLOGY] in Chinese No 4, Apr 78 p 31

[Article by Zhang Chaoguang [1728 2600 0342]: "Influences of Air Temperature and Pressure on Aerial Flights"]

[Text] Aeronautical departments have always regarded high temperature and plateau airfields (low air pressure) as special conditions of aircraft takeoff and landing. Basically speaking, high temperature and low air pressure are direct causes of engine power decline, and lead to decrease in takeoff acceleration as well as the climbing rate of an aircraft after it leaves the ground, which not only decreases the safety of the aircraft, but also makes control difficult. For example, if an agricultural aircraft takes off on a runway 550 meters above sea level at the air temperature of 30 degrees Centigrade, the running distance is almost one half longer than under normal conditions, while the climbing rate is cut down by one third. Thus, agricultural planes are not allowed to operate in plain regions when the air temperature is over 33 degrees Centigrade, or in regions more than 2,500 meters above sea level when the air temperature exceeds 25 degrees Centigrade. This is also why regular airline service planes must reduce their loads at certain air temperatures.

If we disregard the wind at the instant when an aircraft begins to land, we can find the following relation between such factors as touchdown-to-stop distance, air temperature and air pressure with the help of the motion equation of an aircraft taxiing on a runway:

$$L_a = 2GRT/PCySg(-\frac{1}{K} + f)$$

In the above expression. L_a is touchdown-to-stop distance, R is gas constant, P is air pressure, T is absolute temperature, G is aircraft weight, S is wing area, G/S is wing load per unit area (which is a constant if the aircraft type is constant), C_y is lift coefficient, g is gravitational acceleration, K is lift-drag ratio which varies with different types of aircraft, and f is (sliding) friction coefficient.

From the expression, it can be seen that the touchdown-to-stop distance is in direct ratio to wing load per unit area (G/S) and air temperature. The heavier the aircraft and the smaller the wing area are, the longer the running distance is. For instance, the G/S of a C-5 carrier is very small, and its touchdown running distance is also very short; but the G/S of a trident plane is relatively great, and its touchdown-to-stop distance is very long. When the air temperature is high, the air density is low, and the air drag on the plane is also small; thus, the aircraft has to taxi at a longer distance before it can come to a halt. Based on calculations, for each air temperature rise (or drop) of 10 degrees Centigrade, the touchdown-to-stop distances of piston-engine airplanes, turbo-prop planes and jet aircrafts will increase (or decrease) by 5.25 percent, 9.6 percent, and 13 percent respectively. It is worth noting that for a given temperature change in both high air temperature and low air temperature ranges, the results vary only slightly.

The touchdown-to-stop distance and friction coefficient are in inverse ratio to air pressure. The quality of the airfield's runway surface directly affects the running distance of the aircraft taking off or landing. The quality of the runway surface is expressed by the surface sliding friction coefficient: the greater the coefficient, the smaller the running acceleration of the aircraft is, which means that the aircraft needs more time to accelerate, and hence longer running distance. Owing to the difference in runway surface quality, a runway surface with greater friction coefficient makes it necessary for an aircraft to take off at a large angle of attack. Special care must be exercised in the event of ice or sleet on the runway.

When the air pressure is low, the touchdown running distance should be longer. There are dozens of factors causing high or low air pressure in certain areas; among them, the altitude of the airstrip has great influence: i.e. the higher the altitude, the greater the distance the aircraft has to run in order to take off (or land). As the air density over plateau airfields is low, which means that the air pressure is also low, plateau runways are usually much longer than plain runways.

The correct determination of flight altitude is of paramount importance to ensuring flight safety. Thus, the flying altitude of an aircraft over the airfield or in navigational route is usually measured with a pressure altimeter. A pressure altimeter is a kind of instrument used for determining the altitude of a flying aircraft. It is actually a barometer with an aneroid capsule. Based on Hooke's Law, air pressure variations are indicated by the magnitude of spring deformation.

The following formula is often employed by aeronautical departments for calculating altitudes with air pressure values:

$$P_h = P_o \left(\frac{T_o - \Gamma h}{T_o} \right)^{5.253}$$

in which, P_h is air pressure at altitude h , P_o is air pressure at ground level, T_o is ground surface temperature, Γ is average temperature drop rate, and H represents the breadth of the air stratum between P_h and P_o (this formula is only suitable for convection layers).

Based on the above formula, we know that when aneroids are used for measuring altitudes, it is necessary to simplify the expression, i.e. to regard some of the variables in the formula as constants; by common agreement, the International Civil Aviation Organization (ICAO) has set forth the following assumptions: $P_o = 760$ mm, $\Gamma = 0.65$ degrees Centigrade / 100 m, $T = 15$ degrees Centigrade. In the expression, P_h and H are variables, and, based on the formula, P_h may be reckoned in terms of altitude scale H . Moreover, owing to the fact that in practice the atmospheric parameters do not always agree with the three aforementioned hypothetical conditions, it is often necessary to minimize possible errors by adopting the following methods:

Reference setting at mean sea level pressure (QFF) is calculated from the altitude above sea level, field pressure and average temperature measured by the observation post. If the altitude and average temperature (which is usually the mean value of temperatures recorded 12 hours prior to observation) of the air stratum (from ground surface to sea level) are given, and if the altimeter is set to QFF value, the altitude indicated by the altimeter approximates the actual sea level altitude. If the altitude of the air station is 100 meters, and if the metered altitude is likewise 100 meters, then the aircraft is nearing the ground surface. But the error increases if the air station is above 1,000 meters.

Reference setting at positive value (QNH). If the altimeter is on the field surface, and its altimeter indicator is set at the air station's sea level altitude, the altimeter's zero point will correspond to the air pressure value of QNH. This method is based on the assumption that the air column from ground surface to sea level changes with variable Γ in the formula. Its good point lies in the fact that even if QNH is not exactly equal to the actual sea level air pressure, the zero reading of the altimeter on the aircraft is still set at QNH, and when the altimeter indicator approaches the air station's sea-level altitude value, it indicates that the aircraft is nearing the ground surface. Thus, the indicator errors will cancel each other out.

Field Pressure (QFE). When the altimeter's zero point is set at QFE value, the airplane's altitude is approximately equal to the altitude above the field surface.

Zero altitude (QNE). When the altimeter is sitting on the field surface and its zero point is set at 760 mm sea level pressure, its altitude readings are thus in QNE value. When the aircraft is navigating along sea level pressure, and its altimeter reading coincides with the QNE value as reported from the ground surface, it indicates that the aircraft is nearing the ground surface.

Each of the preceding methods have their own merits and demerits. The QFF value will increase with the elevation of the airfield, and the errors will increase as well, which will directly affect the flight safety. Thus, instead of the QFF, airplanes generally adopt the QNH. Moreover, the difference between QNH and QFF should be stressed: While the former is directly measured with the use of a barometric altimeter from the ground surface, the latter is computer from the air pressure and air temperature. Thus, QNH should not be replaced by QFF while in use, otherwise flight accidents will occur.

9119

CSO: 4008

TUBE-TYPE TELEMETRY RAIN GAGE DEVELOPED

Beijing QIXIANG [METEOROLOGY] in Chinese No 4, Apr 78 pp 32-34

[Article by Yuzhixin [0060 3112 0207] of the Production and Technical Division of the Central Meteorological Bureau: "Research on Meteorological Instruments—Tube-type Telemetry Rain Gage (Hyetometer)"]

[Text] Information on rain is closely related to the state economy, the people's livelihood, national defense, and especially agricultural production and water conservancy construction. In order to meet the requirements of meteorological posts which constantly observe raindrops and maintain records of rainfall and rainfall variations, it is highly imperative to study and develop a type of indoor telemetry rain gage (hyetometer) which is not only suitable for continuous use in rainy seasons and rainstorms, but also simple, strong, dependable, accurate, easy to use, and low cost.

In 1977, the Meteorological Bureau of Hebei Province developed a tube-type telemetry rain gage (hyetometer) which was simple, and could be operated from indoors for observing or recording rainfall. Following is a brief description of how the tube-type telemetry rain gage (hyetometer) was developed:

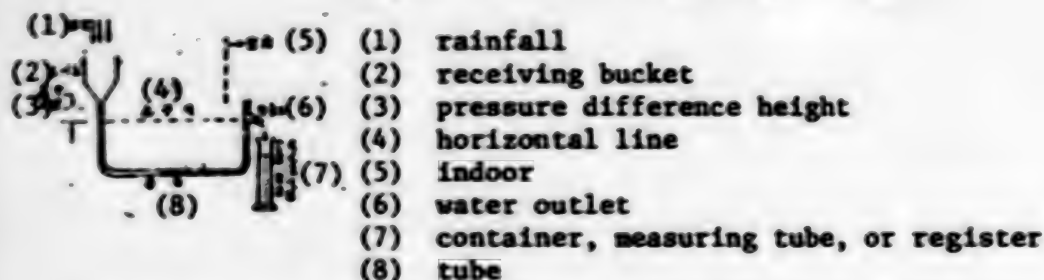
I. Basic Principles

To measure rainfall remotely from indoors, the instrument should meet such technical requirements as being simple, accurate, and easy to operate, which presents a certain amount of difficulty. After comparing various kinds of formulas, it was decided that the adoption of the principle of siphon communicating tubes would be more ideal.

Figure 1 is a schematic diagram showing the application of the siphon communicating tube principle. The receiving bucket is connected to the indoor water outlet via a tube. First, the tube is filled with water, and the water column is adjusted such that the water level is raised to the water outlet of the tube, thus forming a zero-point stationary water level; i.e. the indoor water outlet is on the same horizontal line as the level of the stationary water column in the tube below the outdoor receiving bucket. When a certain amount of water from the bucket drips into the

tube, the level of the water column rises correspondingly above the zero level, and exerts the pressure difference height on the water level at the outlet end, thus forcing water to flow out of the outlet until the water levels at both ends return to equilibrium at the zero-point stationary position. The amount of water discharged from the outlet is equal to the specific quantity of water added to the rain receiving bucket. The rate of flow per unit of time is in direct ratio to the pressure difference height of the water levels, and in inverse ratio to the total impedance of the tube.

Figure 1 Schematic principle diagram



Based on the principle above, if we select the right bucket size, tube diameter, tube length, and water level pressure difference height, it is possible to determine the quantity and variation of rainfall by measuring the quantity and variation of the water flowing out of the tube at the outlet. The volumes of water discharged from the outlet can be observed and recorded with an indoor gage or self-register.

II. How Some Designing Problems are Solved

1. Area of Receiving Bucket Inlet

The inlet area of the rain receiving bucket should be 100 square centimeters (sq cm) which not only economizes on materials and simplifies the manufacturing process, but also enables us to cut down the size, reduce the tube diameter, and increase the length of the tube; it is also suitable for the standard measuring tube, and enables us to employ a 100 sq cm or 500 sq cm siphon hyetometer as the principle device for recording the rainfall. In the manufacturing process, the bucket area should be 100 ± 1.0 sq cm (equivalent to 112.8 ± 0.5 mm in diameter).

2. Tube Diameter, Tube Length, and the Expansion/Contraction Rate of Water Filler

When the tube is filled with water, the water will expand or contract with temperature variation. The diameter and length of the tube should accommodate the instrument tolerance so as to prevent excessive expansion or contraction.

Suppose that the tube volume does not vary with the temperature change. The expansion/contraction rate of the water filler in different tube sizes under temperature conditions of 30 ± 10 degrees Centigrade would be as shown in Figure 2.

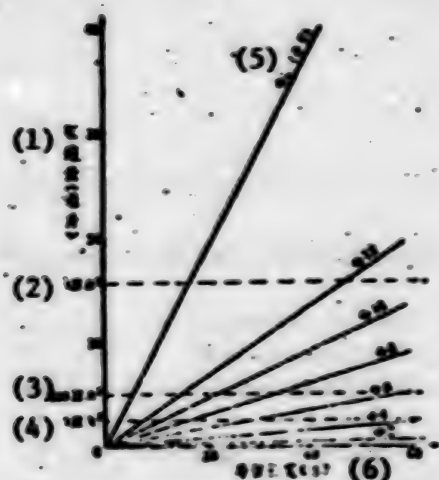


Figure 2 Water filler expansion/contraction rate in different tube sizes

- (1) expansion/contraction rate (ml)
- (2) 314 sq cm
- (3) 100 sq cm
- (4) 50 sq cm
- (5) $\phi 20$ (mm)
- (6) tube length (m)

If the diurnal temperature changes fall within the amplitudinal range of ± 10 degrees Centigrade, the instrument tolerance for the water filler expansion/contraction should not exceed 0.5 mm, and the water filler expansion/contraction rate within the tube of a 100 sq cm receiving bucket should not exceed 5 ml. As shown in Figure 2, if a 5 mm diameter tube is used, its length should not exceed 50 meters.

But when a 5 mm diameter, 50 m long polyvinyl chloride (PVC) soft plastic tube was filled with water and mounted on a frame 2.5 m above the ground level, it was discovered after more than half a month of testing under various natural conditions such as exposure to sunshine, rain, wind, etc., that the expansion/contraction rates of the water filler in the tube and the tube itself were approximately the same, i.e. the discrepancy between the water level variation inside the tube and the rainfall gage could be neglected. Thus, the tube length could be extended from 50 m to 110 m, which was even more suitable for both the accuracy and actual distance requirements of the telemetry instrument.

3. Tube Flow and Water Level Pressure Difference Height

In order to ensure that when there is a strong rainstorm or heavy rainfall the rain water can freely flow from the receiving bucket into the tube and out through the outlet, and to prevent the water from overflowing from the bucket inlet, it is necessary to keep a minimum pressure difference height between the tube inlet at the receiving bucket and the zero-point stationary water level.

The curves in Figure 3 represent the relationship between the flow and water pressure difference height in 5 mm diameter tubes measuring 30 m and 50 m in length.

If the maximum precipitation intensity is determined at 5 mm/min, the maximum flow of a 100 sq cm bucket tube should be 50 cubic cm/min. From the test curves in Figure 3, it can be seen that if the tube diameter is 5 mm, and its length is 30 m, then the pressure difference height should not be less than 152 mm; if the tube is 50 m long, the pressure difference height should not be less than 10 mm. It is thus estimated that the pressure difference height of a 100 m tube should not be less than 430 mm.

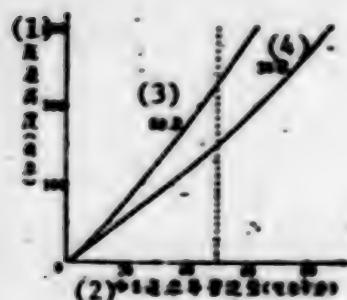


Figure 3 Ø5 mm diameter tube flow and pressure difference height

- (1) pressure difference height (mm)
- (2) Ø5 mm tube flow (cubic cm per minute)
- (3) 50 m
- (4) 30 m

4. Measuring and Recording Rainfall Indoors

When it rains, the rain water flowing out of the tube outlet into the room can be measured with a 500 ml measuring tube: Each 10 ml volume of rain water is equivalent to 1 mm rainfall. A hand balance or platform balance may also be used: Each 1/5 liang (1 liang = 50 grams) or 10 grams is equivalent to 1 mm rainfall.

A vessel is placed beneath the measure tube. The vessel capacity should be 1,000 ml, and can be used to retain water overflowing from the measuring tube, and thus prevent loss of water due to evaporation.

To record rainfall and its variation with self-registering devices, a 130 sq cm or 500 sq cm siphon rain gage is installed indoors at the tube outlet, and is used as the main recording equipment. It can siphon 50 mm of rainfall at a time. Thus, it is now possible to operate the siphon rain gage indoors instead of installing the system outside on the observation ground where one would have to conduct observations, change paper, adjust and maintain the instruments in the wet rain.

5. Instrument Measurement Errors:

The primary factors causing errors in combination instruments are: The tolerance allowed in the manufacturing process of the rain receiving bucket inlet area; the expansion/contraction rate of the water filler in the tube due to temperature changes; the amount of remnant rain water adhered to the

rain receiving bucket and filter; the level-drop of water in the tube caused by evaporation; as well as measuring tube error. From preliminary studies, the accuracy of this type of telemetry rain gage is as follows:

0.6 mm when the rainfall does not exceed 30 mm;

2% x rainfall when the rainfall exceeds 30 mm

If a certain degree of accuracy is required in determining or checking the size of very small precipitation, a 50 sq cm rain gage can be linked to the system.

6. Installation

The indoor tube outlet should be placed at a height which is convenient for observation and operation, and the height of the outdoor rain receiving bucket is adjusted accordingly. To prolong the lifespan of the plastic tube, it is necessary to protect it from the radiation of the sun by burying it at a certain depth below the ground surface, or by covering it with sand, fine earth, bricks, tiles, bamboo pieces, bamboo pipes, hard plastic pipes or with whatever is available. If the system is to be temporarily installed for special jobs, the tube can be suspended like cables with wooden poles or bamboo poles. But whether it is buried underground or suspended in mid-air, the entire length of the tube must be kept tubular when in use; it should not be bent, folded, flattened or deformed in such a way as to obstruct the water flow inside the tube. In winter, when water freezes, the water inside the tube should be removed; the tube should be cleaned and the ends of the tube should be protected.

7. How to Prevent Tube Clogging

If dust or sand fall into the funnel of the rain receiving bucket, and the rain water flushes them down into the tube opening and the tube itself, or if bubbles or air columns are arrested inside the water column in the tube, or if a water column or bubble should form within the "pressure difference height" section of the tube when the rain water flows into the tube from the receiving bucket, the water flow inside the tube will be hampered and thus cause measurement errors or instrument malfunction.

Thus, in designing the system, the funnel tubes of the receiving bucket and water inlet funnel should protrude 5-9 mm above the end of the funnel cones so as to allow dust and sand particles which are not bigger than 3 cubic cm to deposit inside the cone troughs of the two funnels. By adding a filter mask over the inlet funnel, relatively large pollution particles can be prevented from entering the tube. A filter is installed below the zero-point stationary water position to prevent relatively large dust, sand and pollution particle from entering the tube.

The "pressure difference height" tube between the inlet funnel and filter should be 7-9 mm in diameter, and not too small. In addition, two clean 20# copper threads or lead threads are inserted from the inlet funnel filter mask into the tube and to the filter; this can eliminate and prevent water columns and air bubbles from forming when rain water starts to enter the tube.

When filling the tube, the water should be continuously poured into the inlet funnel so as to remove all the bubbles from within the tube.

As the two tube sections below the receiving bucket and indoor water injector frequently move, they should be made of rubber so as to prevent the tube passages from bending and deforming.

8. Compensating the Evaporation on the Water Surface in the Tube

As the evaporation occurs at the surface of the water in the tube, the zero-point stationary water position will gradually fall and thus affect the accuracy of rain measurement. In order to avoid the trouble of adding water every few days, an automatic water injector was designed and installed above the water outlet (see Fig. 4). The automatic injector is composed of an injection syringe and auto-injection flask. The flask is filled with clean water, and inserted upside down into the injection syringe; the opening of the flask should be placed at the lowest water level. When the water surface falls below the flask opening, the flask automatically lets out water, thus restoring the water level to its original position. The water inside the injection flask can compensate 20 ml of evaporated water, which means that a full flask can last 1-3 months, and within this period, there is no need to manually add water.

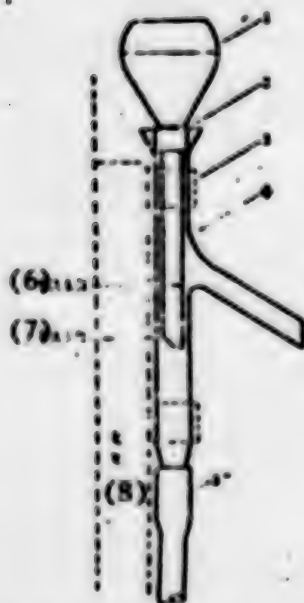


Figure 4 Automatic water injector

- (1) auto refill flask
- (2) rubber tube
- (3) tube fastener
- (4) injection syringe
- (5) rubber tube
- (6) zero-point water level
- (7) lowest water level
- (8) support frame

The minimum water level is determined by the diurnal expansion/contraction rate of the water filler in the tube caused by temperature changes, i.e.

the diurnal maximum expansion rate should not cause the water surface to become higher than the rain water level, which will prevent the water from overflowing out of the tube when there is no rain. The minimum water level can be regulated by adjusting the position of the rubber tube above the flask.

Figure 5 is a schematic diagram of the structure and position of the telemetry rain gage (hyetometer).

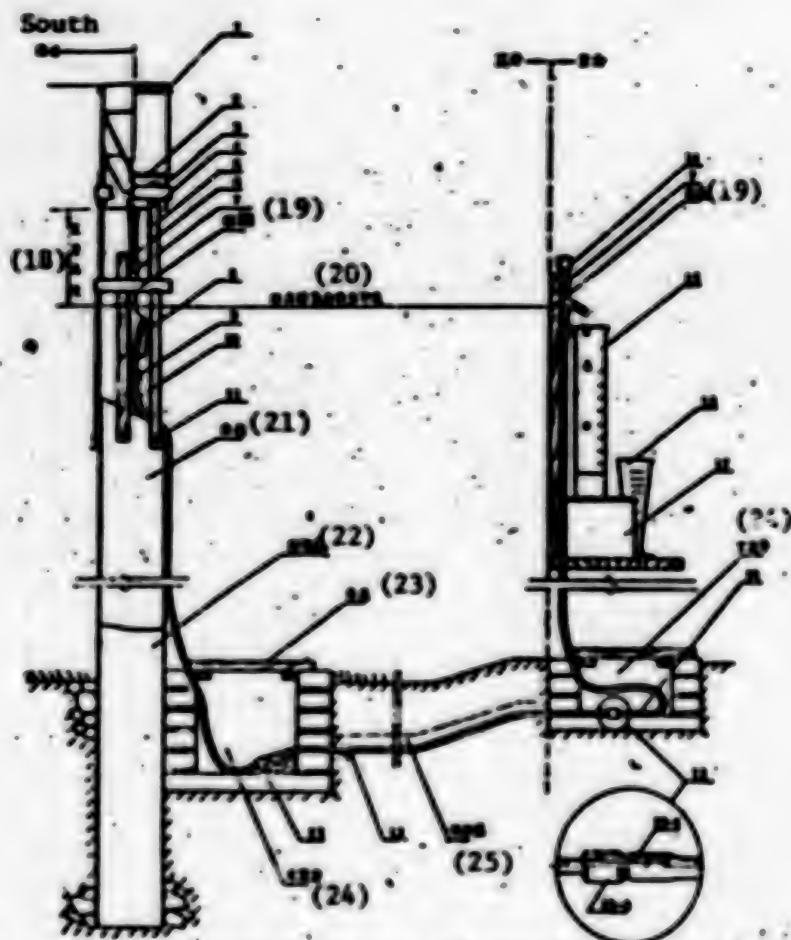


Figure 5 Schematic diagram of the telemetry rain gage (hyetometer)

- | | |
|-------------------------------------|---|
| 1. 100 sq. cm rain receiving bucket | 14. injector |
| 2. filter mask | 15. measuring tube |
| 3. water inlet funnel | 16. measuring cup |
| 4. fixation screw | 17. water receiving vessel |
| 5. support frame | 18. pressure difference height |
| 6. rubber tube | 19. board frame |
| 7. tube fastener | 20. zero-point stationary water level horizontal line |
| 8. dust filter | 21. wooden pile |
| 9. wood screw | 22. rust-proof coat |
| 10. rubber tube | 23. wooden lid |
| 11. wood screw | 24. placement pit |
| 12. tube joint | 25. protective layer |
| 13. plastic tube | |

If the indoor water outlet is connected to the registering device of a 100 sq cm or 500 sq cm siphon rain gage, the indoor installation should be as shown in the schematic diagram in Figure 6.

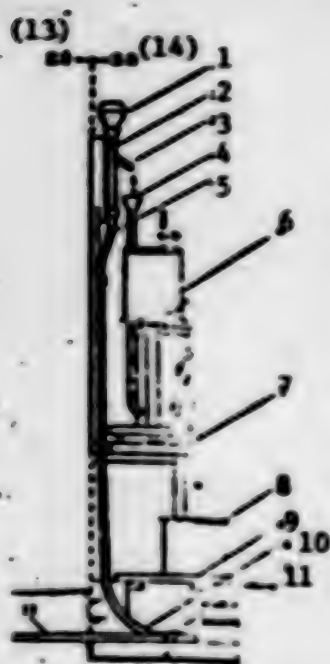


Figure 6 Installation of indoor self-registering system

1. auto-filling flask
2. tube fastener
3. injection syringe
4. water inlet of float chamber
5. wall fixation board
6. main unit of siphon rain gage
7. support frame for main unit installation
8. water storage vessel
9. wooden lid
10. $\varnothing 8$ rubber tube
11. tube joint
12. $\varnothing 5$ plastic tube
13. outdoor
14. indoor

III. Preliminary Test Results

From July through October last year, preliminary comparative tests were carried out by the Cangzhou Meteorological Station, the Linxi County Meteorological Station, the Biegu Village Middle School in Yongqing County, the Beishang Meteorological Post in Rongcheng County, and the Baoding Instrument Supply Station respectively. Results of the comparative observations are shown in the appendix table.

Appendix Table

(7) 项目		(1) 地点	(2) 日期	(3) 项目	(4) 日期	(5) 项目	(6) 日期
(8) 地点		1. 地点		2. Linxi		3. Cangzhou	
(9) 日期		4. Biegu Village		5. Beishang		6. Baoding	
(10) 项目		7. item		8. date		9. tube length (m)	
(11) 管长 (m)		10. comparative frequency		11. total rainfall (mm)		12. tube total rain water measure (mm)	
(12) 比较次数		13. total comparison difference (mm)		14. mean comparison difference (mm)			
(13) 总雨量 (mm)							
(14) 平均比较差 (mm)							

The Hebei Provincial Meteorological Bureau is conducting further experiments to improve the instrument.

CLIMATIC CONDITIONS CAUSING WHEAT SCAB DISEASE OUTLINED

Beijing QIXIANG [METEOROLOGY] in Chinese No 4, Apr 78 pp 35-37

[Article by the Operation Division, Shanghai Meteorological Bureau:
"Climatical Conditions Causing Wheat Scab Disease"]

[Text] Cereal scab is the major disease of wheat species. Each year in the Shanghai suburban area, the three wheats [naked barley, barley, wheat] are affected to various degrees by this kind of disease, which is the chief factor affecting the stable yield and high yield of summer grain crops. In order to improve meteorological forecasting of the three wheat scab disease weather, and meet the needs of scientific farming, this article will present a preliminary analysis of the relationship between the outbreak of cereal scab disease, the degree of harm and damage, and climatic conditions based on data from related agricultural scientific experiments.

In the Shanghai region, when the three wheats enter the earing, flowering, filling and milking stages each year from mid-April to mid-May, it is also the heaviest spring rain season. During this period, the air temperature gradually rises, and the mean air temperature generally ranges from 14 to 18 degrees Centigrade. As the weather is mostly hot and wet, it often becomes the major epidemic period of the cereal scab disease in the city. From the past outbreak periods of the three-wheat scab disease in the Agricultural Bureau's Plant Protection Station, which is located in Fengxian County, Shanghai City (see Table 1), it is plain that the naked barley scab disease occurs mostly in mid and late April, and becomes acute from late April to early May; the wheat scab disease occurs mostly from late April to early May, and becomes acute in early and mid May. Due to the different annual meteorological conditions, the number of interval days between the disease outbreak and acute stage may vary. In years of high incidence, there are 5-7 days between the outbreak and acute stage; in slow years, there are 10-15 days in between.

Table 1 The outbreak periods of the three wheats scab disease over the past years in Fengxian County, Shanghai City

(1) 年 份	(2) 元 大 麦				(3) 小 麦			
	始(4)月		至(5)月		始(4)月		至(5)月	
	(6) 日	(7) 日	(6) 日	(7) 日	(6) 日	(7) 日	(6) 日	(7) 日
1955	4	29-30	5	13	5	1-4	5	8-10
1956	4	26-29	5	8	5	1-4	5	9-12
1957	4	26-30	5	7	5	12-14	5	17-19
1958	4	21-25	4	28	4	25	5	5
1959	4	17	5	1	4	22	5	2
1960	4	15	4	28	4	17-20	4	30
1961	4	17	4	28	4	25	5	15
1962	4	21-25	5	5	4	29	5	19-21
1963	4	21	4	28	5	5-8	5	14-17
1964	4	22-26	5	4	4	30	5	11
1965	4	22-27	5	1-5	5	5	5	11
1966	4	16-18	4	23	4	27	5	12
1967	4	23	4	28	5	11	5	1
1972	5	4	5	9	5	11	5	19
1973	4	14	4	17	4	26	5	7
1974	4	30	5	9	5	11	5	19
1975	4	30	5	6	5	5	5	20
1976	4	25	5	8	5	8	5	19
1977	4	30	5	19	5	10	5	15

有 * 者为原来的发病期 (8)

- (1) year (5) acute stage
 (2) naked barley (6) month
 (3) wheat (7) day
 (4) outbreak (8) asterisk (*) represents original outbreak period

Due to the fact that in each given year there are different cereal scab disease sources, epidemic growth periods, cultivation measures, and meteorological conditions, the degree of the cereal scab disease outbreak varies greatly from year to year. But case histories of the disease over the past years indicate that the decisive factor lies in the meteorological conditions. In this article, we will analyze the following problems:

1. The Critical Periods of the Occurrence and Spreading of the Disease

Generally speaking, the flowering stage coincides with the disease infection period, and the filling and milking stages coincide with the outbreak stage of the disease. But due to the change of weather and climatic conditions from year to year, the infection and growth periods also differ each year,

and there is a relatively great distance between the time of occurrence and the time of spreading. For example, in 1972, the outbreak of the naked barley disease occurred on 4 May; but in 1973, it took place on 14 April, which was 20 days later. The primary cause of this kind of discrepancy lies in the fact that the infection and development stages of the disease (i.e. earing and flowering) in 1973 was half a month earlier than 1972.

If we look into the three wheat growth data over the past few years and combine it with analysis of the climatic data, we will find that when the three wheats are properly sown, the earing and flowering periods may vary with the variations of winter/spring temperatures, and the distance between sowing and earing may be as great as 10-odd days; but the effective accumulative temperatures above 3 degrees Centigrade required during the sowing and earing periods each year are relatively stable with very little fluctuations. For example, the effective accumulative temperature required for the wheat variety Yangmai No 1 is approximately 840 degrees Centigrade (from sowing to full heading); for the barley variety Zaoshu No 3, it is approximately 620 degrees Centigrade; and for Naked Barley No 757, it is 560 degrees Centigrade. These figures indicate that the progress rate of the three wheats' growth periods is chiefly related to the amount of accumulative temperature in winter and spring of the same year. Figure 1 shows that there is a clear correlation between the effective accumulative temperatures of winter and spring and the timing of the full heading and disease outbreak stages. If there is a great amount of effective accumulative temperature in winter and spring, the full heading stage occurs early, and, correspondingly, the cereal scab disease occurs ahead of time. Conversely, if the full heading stage is delayed, the disease outbreak will also be slightly delayed. The three curves in the figure basically follow the same rise-and-fall pattern, which fully indicates that the magnitude of the effective accumulative temperatures above 3 degrees Centigrade in winter and spring can fairly accurately reflect when the three wheats are infected by the disease, and when the disease outbreak occurs. Therefore, to predict and forecast the cereal scab disease, it is necessary to analyze the year's winter/spring accumulative temperature conditions, and thus accurately determine which infection period is most critical to the outbreak of the disease.

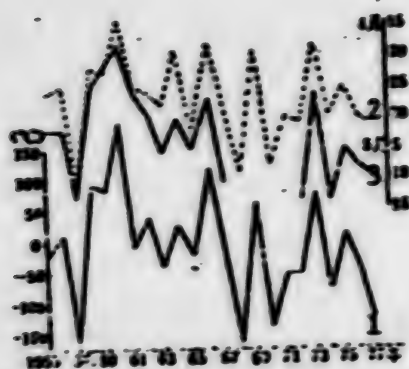


Figure 1 Curves of winter/spring effective accumulative temperatures, wheat full heading periods, and disease outbreak periods over the past years.

- Curve (1):** Anomaly values of effective accumulative temperatures above 3 degrees Centigrade (averages 566 degrees Centigrade in the average year) from mid-November of the preceding year to late March.
- Curve (2):** Full heading periods of wheat variety Yangmai No. 1 from 11 November when it was sown (calculations based on 840 degrees Centigrade accumulative temperatures above 3 degrees Centigrade from sowing to full heading).
- Curve (3):** Wheat disease outbreak periods (based on Table 1); the ordinates represent the anomaly values of the effective accumulative temperatures above 3 degrees Centigrade ranging from mid-November of the preceding year to late March.

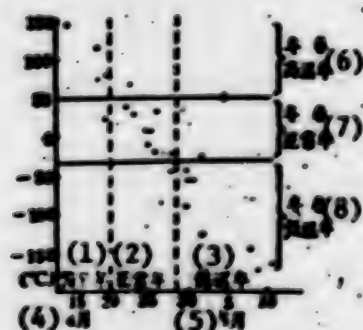


Figure 2 Diagram showing relationship between winter/spring accumulative temperatures and full heading periods (1955-1977)

Ordinates represent mean values of winter/spring effective accumulative temperatures; Abscissas represent wheat full heading periods.

- | | |
|-----------------|-------------------------------|
| (1) early year | (5) May |
| (2) normal year | (6) warm winter/spring year |
| (3) late year | (7) normal winter/spring year |
| (4) April | (8) cold winter/spring year |

In order to determine the critical infection periods of each given year, we divided the winter/spring effective accumulative temperatures into three climatic categories in accordance with the dates of the wheat full heading stage (Figure 2): In the first category, the wheat full-heading stage comes slightly earlier (before 20 April) for 5 years, including 4 years of accumulative temperature anomaly values greater than +50 degrees Centigrade, which constitute warm winter/spring years. In the second category, the full-heading period is normal (from 21 to 28 April) for 9 years; including 8 years of accumulative temperature anomaly values ranging between +50 to -30 Centigrade, which constitute normal temperature winter/spring years. In the third category, the full-heading stage is slightly delayed (after 29 April) for 9 years; including 8 years of accumulative temperature anomaly values less than -30 degrees Centigrade, which constitute cold winter/spring years. In accordance with the three types of winter/spring climate years, we made statistical calculations of the average full heading periods of the three wheats over the recent years (based on accumulative temperatures), and the average outbreak and acute growth periods of the cereal scab disease, as shown in Table 2. The table plainly indicates that owing to the different winter/spring accumulative temperature conditions, the full-heading periods and disease outbreak periods do not coincide, but the time of their occurrence is delayed in accordance with the winter/spring accumulative temperature variations, and the number of interval days between the full heading and disease outbreak follow a relatively set pattern. For example, on the average, the disease outbreak of naked barley occurs in the 2nd or 3rd seasonal period following the full heading stage, and the average acute disease stage occurs in the 4th or 5th seasonal period following the full heading stage. In the case of wheat, the average disease outbreak stage occurs in the 1st seasonal period following the full heading stage, and the average acute disease stage is in the 3rd or 4th seasonal period following the full-heading stage. Based on the above pattern, and combining it with the fact that in an average year there are approximately 7 interval days between the acute growth stage and the epidemic stage of the cereal scab disease, we have found that the critical period which is most conducive to the outbreak and spreading of the wheat disease is generally about one month or so. Thus, Table 3 shows the initially determined critical periods of the different winter/spring climates which are most closely related to the degree of disease outbreak. Thus, in early April, based on the amount of winter/spring accumulative temperature, it is possible to make initial estimation of when the disease will occur in the year, and which weather period is most related to the spreading of the disease.

Table 2 Mean full-heading, disease outbreak and acute development periods in an average year under different winter/spring accumulative temperature conditions in Shanghai

(1) 品种	(4) 冬/春季 气候类型	(8) 3月		(9) 4月						(10) 5月				
		28-31	1-5	6-10	11-15	16-20	21-25	26-30	1-5	6-10	11-15	16-20		
(2) 元大麦	高温年 5	齐穗			始病		(13)		(13)					
	正常年 6	(11)		齐穗	(12)	(11)	始病	(12)	盛发	(13)				
(3) 小麦	低温年 7					齐穗	始病			盛发	(13)	(13)	(13)	(13)
	正常年 6					(11)	齐穗	始病	(11)	(13)	盛发	(13)	盛发	盛发
	低温年 7						(11)	(12)	齐穗	(12)	盛发	(12)		

- | | |
|--------------------------------|--------------------------------------|
| (1) variety | (8) March |
| (2) naked barley | (9) April |
| (3) wheat | (10) May |
| (4) winter/spring climate type | (11) full heading |
| (5) high temperature year | (12) disease outbreak |
| (6) normal temperature year | (13) disease acute development stage |
| (7) low temperature year | |

Table 3

(1) 品种	(5) 上年11月中旬至3月下旬>3℃有效积温距平值	(7) 元大麦关键期	(13) 小麦关键期
(2) 高温年	(6) >615℃ (距平>+50℃)	(8) 4月6日-5月6日	4月6日-5月10日 (11)
(3) 正常年	(6) 615℃-435℃ (距平+50℃--30℃)	(9) 4月11日-5月10日	4月16日-5月15日 (10)
(4) 低温年	(6) <435℃ (距平<-30℃)	(10) 4月16日-5月15日	4月21日-5月20日 (12)

- | | |
|--|----------------------------------|
| (1) winter/spring climate type | (6) anomaly |
| (2) high temperature year | (7) naked barley critical period |
| (3) normal year | (8) 6 April to 5 May |
| (4) low temperature year | (9) 11 April to 10 May |
| (5) effective accumulative temperatures above 3 degrees Centigrade and mean anomalous values from mid-November of the preceding year to late-March | (10) 16 April to 15 May |
| | (11) 6 April to 10 May |
| | (12) 21 April to 20 May |
| | (13) wheat critical period |

II. Climatic Conditions Causing Outbreak and Spreading of the Disease

We have analyzed 17 years of climatic conditions prior to the wheat disease outbreaks. Although the conditions of each year are relatively complicated, there are three basic types of climate based on the climatic conditions 10 days prior to the disease outbreak. (See Table 4)

Table 4 Climatic conditions 10 days prior to disease outbreak in various typical years

(1) 气候类型	(2) 年份	(3) 发病前10天的气候条件		(6) 总降雨量 (mm)	(8) 发病率 (%)	(9) 等级
		(4) 平均气温 >15°C 天数	(5) 相对湿度 >80% 天数			
(10) 高温高湿	1973	8	7	8	30.0	重(14)
(11) 多雨年	1977	7	8	8	101.2	重(14)
(10) 高温高湿	1966	7	8	4	33.8	中(15)
(12) 少雨年	1976	8	7	4	33.2	中(15)
(13) 低温高湿	1966	2	8	7	67.2	轻(16)
(11) 多雨年	1967	2	8	8	46.4	轻(16)

- (1) type of climate 10 days prior to the disease outbreak
- (2) typical year
- (3) climatic conditions 10 days prior to disease outbreak
- (4) number of days in which the mean air temperature $> 15^{\circ}\text{C}$
- (5) number of days in which the relative humidity $> 80\%$
- (6) total rain days
- (7) total rainfall (mm)
- (8) percentage of disease-stricken wheat ears (I)
- (9) degree of disease
- (10) high temperature high humidity
- (11) abundant rainfall year
- (12) low rainfall year
- (13) low temperature high humidity
- (14) serious
- (15) medium
- (16) light

The first type is called high temperature high humidity abundant rainfall year. In this type of year, the air temperature is high, there are many wet days, the humidity is high, the mean air temperature is generally above 15 degrees Centigrade, and the mean relative humidity is above 85 percent, which constitute the most favorable conditions for the outbreak and spreading of the cereal scab disease. Most of these years are hit by serious epidemic cases, such as 1973 and 1977. The second type is known as high temperature high humidity low rainfall year. Prior to the disease, there are not many

wet days, but the spring is mostly foggy or cloudy, the air temperature is high, the humidity is high, and the epidemic rate during such years is usually medium, e.g. 1966, 1976. The third type is the low temperature high humidity abundant rainfall year. The mean temperature is below 14 degrees Centigrade; due to continuous cloudy and wet weather, the humidity is high, and the mean relative humidity is constantly above 85 percent. Most of these years are hit by light epidemic cases, such as 1960 and 1962.

It can be seen from the relationship between the three types of climate and the epidemic degree that: (1) Prior to the disease outbreak, some are low temperature years, some are low rainfall years, but their common feature lies in the high air humidity. Evidently, high air humidity is the most important climatic factor leading to the outbreak and spreading of the cereal scab disease. Under suitable humidity conditions, high temperatures can become a major condition which accelerates the development of the disease. (2) There is also a certain relationship between the different types of pre-epidemic climates and the degree of calamity. This is due to the fact that the meteorological conditions 10 days prior to the disease outbreak often reflect the climatic features of spring. For instance, in 1977, before the outbreak of the epidemic, the weather was hot, humid and wet; after the outbreak, it continued to be hot, humid and wet. Thus, if we make timely analysis of the meteorological conditions prior to the epidemic outbreak, it helps us to keep abreast of the growth trend of the epidemic in its later period.

III. Statistical Analysis of Epidemic Climate Indices

At present, to a great extent, the prediction of the degree of cereal scab epidemic is based on many years of weather forecasting. In order to make full use of the long term weather forecasts, we must set up certain types of climatic indices that are simple but strongly correlated to the cereal scab disease. Based on the information provided by the Shanghai Academy of Agricultural Sciences which revealed cases of wheat scab diseases over the past years, we divided the degree of epidemic growth into three grades (see Table 5).

Table 5 Grade schedule of cereal scab disease incidences

Grade of epidemic growth	Incidence (%)	Degree of epidemic growth
1	0 - 20	light
2	21 - 50	medium
3	>50	serious

We compared the climatic conditions of each year, and through correlative statistical computation of different combinations of meteorological factors, we have found that the type of combination which is relatively correlated to

the degree of epidemic growth is the one which includes temperature and humidity (see Table 6); and the best correlative combination occurs in warm and humid days, especially when the mean air temperature is ≥ 15 degrees Centigrade, and the relative humidity is ≥ 85 percent. For instance, based on the preceding critical periods which are divided according to different winter/spring accumulative temperatures, we made statistical calculations of the total number of days in which the various meteorological factor combinations appeared in each given year, and the results are shown in Table 7. From the table, we can see the following: There are 7 light epidemic years in which the number of warm humid days with the combination of mean air temperature $\geq 15^{\circ}\text{C}$ and mean relative humidity $\geq 85\%$ are ≥ 8 , which conform to the 1st Grade in the schedule of wheat epidemic degrees; there are 9 medium epidemic years in which there are 9-12 days, which conform to Grade 2; there are 5 years in which there are ≥ 13 days, including 3 years which conform to Grade 3, i.e. grave epidemic years, and 2 years are medium epidemic with 1 grade less. Out of 21 years, there are 19 years in which the number of warm humid days that appeared in the critical period matched exactly with the wheat epidemic grades. There is a difference of 1 grade in every 5 years for the other two kinds of factor combinations. Hence, the comparatively ideal index for forecasting cereal scab epidemic climate is the number of warm humid days with the combination of mean air temperature ≥ 15 degrees Centigrade and mean relative humidity ≥ 85 percent.

Table 6 Correlation between degrees of epidemic growth and various meteorological factor combinations

(1) 分类	(2) 相关系数 (R)	(3) 各种组合		
		(4) 平均气温 $\geq 15^{\circ}\text{C}$ 相对湿度 $\geq 85\%$ 的暖湿天数的 暖湿天数	(5) 平均气温 $\geq 15^{\circ}\text{C}$ 相对湿度 $\geq 80\%$ 的暖湿天数的 暖湿天数	(6) 平均气温 $\geq 15^{\circ}\text{C}$ 的 湿日天数
(7) 发病率计算		+0.79	+0.75	+0.70
(8) 发病率等级计算		+0.85	+0.78	+0.65

- (1) category
- (2) correlation coefficient (R)
- (3) various combinations
- (4) warm humid days with combination of
mean air temperature ≥ 15 degrees Centigrade
relative humidity ≥ 85 percent
- (5) warm humid days with combination of
mean air temperature ≥ 15 degrees Centigrade
relative humidity ≥ 80 percent
- (6) wet days with mean air temperature ≥ 15 degrees Centigrade
- (7) calculations based on rate of disease-stricken ears
- (8) calculations based on grade of epidemic growth

Table 7 Verification results showing wheat epidemic grades and number of days in which various meteorological factor combinations appeared

(1) 年 份	(2) 麦		(3) $\bar{T} \geq 15^{\circ}\text{C}$ and $\bar{H} \geq 85\%$ 的天数				(4) $\bar{T} \geq 15^{\circ}\text{C}$ and $\bar{H} \geq 80\%$ 的天数				(5) $\bar{T} \geq 15^{\circ}\text{C}$ 的日数				(6) 估计值	
	a	b	a	b	c	d	a	b	c	d	a	b	c	d	a	b
1957	35	2		12		<		15		<		12		<	2	<
1958	60	3	13			<		16		21级	15	12		<	3	<
1959	25	2		12		<		15		<		9		<	2	<
1960	5	1			5	<			7	<			6	21级	1	<
1961	5	1			8	<			13	<		9		21级	1	<
1962	15	1			8	<			9	<			7	<	1	<
1963	35	2	14			21级		16		<		11		<	3	21级
1964	35	2		12		<	17			21级			5	21级	2	<
1965	15	1			8	<			13	<			7	21级	1	<
1966	25	2		9		<			12	21级			6	21级	2	<
1967	45	2		11		<		14		<		12		<	2	<
1968	15	1			5	<			12	<			3	<	1	<
1969	25	2	13			21级		16		<		9		<	3	21级
1970	25	2		11		<			13	21级		9		<	2	<
1971	10	1			5	<			12	<		10		21级	1	<
1972	35	2		12		<			12	21级		10		<	2	<
1973	60	3	13			<	13			<	13			<	3	<
1974	5	1			7	<			11	<		11		21级	1	<
1975	25	2		11		<		16		<		10		<	2	<
1976	35	2		9		<		15		<		10		<	2	<
1977	60	3	11			<	18			<	13			<	3	<

Note: Wheat disease incidence data from Shanghai Academy of Agricultural Science

- (1) year
- (2) wheat
 - (a) epidemic incidence (%)
 - (b) epidemic grade
- (3) number of days in which $\bar{T} \geq 15^{\circ}\text{C}$ and $\bar{H} \geq 85\%$
 - (a) >13 days, grade 3
 - (b) $12-9$ days, grade 2
 - (c) <8 days, grade 1
 - (d) verification
 - (e) 1 grade less
- (4) number of days in which $\bar{T} \geq 15^{\circ}\text{C}$ and $\bar{H} \geq 80\%$
 - (a) >17 days, grade 3
 - (b) $16-14$ days, grade 2
 - (c) <13 days, grade 1
 - (d) verification
 - (e) 1 grade less
- (5) number of wet days in which $\bar{T} \geq 15^{\circ}\text{C}$
 - (a) >13 days, grade 3
 - (b) $12-19$ days, grade 2
 - (c) <8 days, grade 1
 - (d) verification
 - (e) 1 grade less
- (6) \bar{y} estimated value
 - (a) epidemic grade
 - (b) verification
 - (e) 1 grade less

The closest correlation that ever occurred between the wheat scab disease incidence and warm-humid combination of mean air temperature ≥ 15 degrees Centigrade and mean relative humidity ≥ 85 percent appeared in 1957-1977. Based on the preceding information and on the principle of the lowest (binomial multiplication), we used the straight line regression equation $\hat{y} = a + bx_1$ and computed $a = -18.66$, $b = 4.65$, from which we derived the estimation: $\hat{y} = -18.66 + 4.65x_1$. x_1 is the number of warm humid days in the critical period; \hat{y} is divided into three zones which indicate different epidemic growth grades:

≥ 20 is Grade 1 (light epidemic year)

21 - 40 is Grade 2 (medium epidemic year)

≥ 41 is Grade 3 (grave epidemic year)

The epidemic growth grades based on the \hat{y} values of each year are listed in Table 7; their similarity rate is relatively high.

9119

CSO: 4008

DITCHES USED TO PREVENT MOISTURE FROM HARMING THREE WHEATS

Beijing QIXIANG [METEOROLOGY] in Chinese No 4, Apr 78 p 38

[Article in special section "Swapping Experiences Among Meteorological Posts" by Chonggu Middle School Meteorological Post, Qingpu County, Shanghai: "Proper Use of Ditches to Prevent Moisture from Harming the Three Wheats"]

[Text] South of the Yangtze River, spring is a comparatively rainy season and the soil becomes overly wet, causing maldevelopment in the root systems of the three wheats [barley, wheat and naked barley], which gives rise to early deterioration, many diseases, lodging and "dead ripeness", thus affecting the crop yield. As Qingpu County is situated in a low-lying area, it is susceptible to worse moist calamities. In recent years, an effective method for preventing moisture calamity has been developed by digging a system of ditches in wheat fields. But how can the ditches be scientifically arranged so as to combine with such local conditions as soil texture, relief and climate? How can we save labor and time, achieve good results, avoid delaying agricultural work, and turn it to the advantage of producing high yields at the same time? In 1976, we made some experiments.

The experiment was divided into two sections: one section consisted of three different forms of ditches—open drain, underground drain and open/underground drain—for comparison purposes. The other section consisted of ditches placed 3 meters, 4 meters, 5 meters and 6 meters apart from each other, also for comparative experimentation. The total acreage of the experimental plot was 17 mu [1.1339 hectares], and "Early Ripe No 3" wheat was chosen as the experimental variety. The sowing time of one group was 10 November, and other group was 16 November. The rate of seeding was set at 35 jin [17.5 kilograms] per mu [0.0667 hectares].

1. The Water Drainage and Reduction Capability of Different Forms of Ditches

The comparative experimentation of open drains, underground drains and open/underground combined drains was carried out in three juxtaposed plots,

3 m each. The large 0.9 meter deep open drains were dug along the northern and southern sides of the experimental plot. The ditches in the field were placed 4 meters apart. In the open drain plot and open/underground drain plot, transversal ditches were dug 15 meters apart with banks; open drains were 1.5 meters deep, and underground ones were 2.4 meters deep. The open and underground ditches were arranged between each other.

Experimental results showed that in all three forms of drainage methods, the moisture of soil layers below 20 cm remained saturated, and there were no evident differences among them. But at 0-20 cm active soil layers, the soil moisture variation became evident: open drains and open/underground combined drains could effectively remove ground surface water and subterranean water, but underground drains proved relatively poor. For example, on 1-3 January 1977, there was a total of 15 mm of rainfall, and measurements made on 6 January showed the following: the soil moisture at 10 cm was the smallest in the open drain plot, and the results of open/underground combination drain plot was second best; the soil moisture at 20 cm was the smallest in the open/underground drain plot, and underground drain plot ranked second. On 7-9 January that year, there was 16 mm of rainfall, and the results of measurements made on 10 January were the same. In continuous precipitation, such as 15-30 January, there was a continuous rainfall of 46 mm which lasted half a month, and measurements made on 3 February showed that the drainage capability of open/underground combined drains as well as open drains alone were better than underground drains (see Table 1).

Table 1

Year: 1977

(1) 日期 (2.1.8)	(2) 1月6日			(3) 1月10日			(4) 2月3日		
(5) 深度 (cm)	0-5	10	20	0-5	10	20	0-5	10	20
0-5	23	37	36	34	43	45	36	29	37
10	30	43	47	39	47	53	43	33	47
20	44	33	37	41	36	34	30	20	44
30	27	37	37	38	36	38	25	36	36
40	27	37	37	38	36	38	25	36	36
50	25	29	30	38	36	38	27	27	31
60	25	29	32	38	36	38	27	27	31

(1) measurement date

(2) 6 January

(3) 10 January

(4) 3 February

(5) depth (cm)

(6) open drain

(7) open/underground drain

(8) underground drain

2. The Water Drainage and Moisture Reduction Capability of Drains With Different Spacings

The experimentation of open/underground combined drains was carried out in four plots (2 m each). Experimental results showed that the water drainage

and moisture reduction capability of ditches placed 3 or 4 meters apart were the best, and that the capability dropped considerably in spacings of 5 or 6 meters. For example, on 22-25 December 1976, there was a rainfall of approximately 30 mm; 5 days later, soil moisture measurements were made at various depths and tabulated as shown in Table 2. From this table, it can be seen that 4 meter spacing was the best.

Table 2 Soil Moisture (X) of Wheat Fields With Different Drain Spacing After Rain

(1) (2)	0-2	10	20	30	40	50	60
3	30	30	33	37	38	37	25
4	31	34	38	36	36	27	26
5	34	40	38	38	32	23	27
6	40	40	39	32	27	20	27

(1) Depth (cm)
(2) Spacing (m)

The results of the experiments indicate that in regions south of the Yangtze River which abounds in spring rain, the proper and effective way of preventing and controlling wheat field moisture calamity is by digging open or open/underground ditches placed 4 meters apart; the open drains should be 1-1.5 chi [0.3-0.5 meters] deep, underground drains should be 2.4 chi [0.7 meters] deep; moreover, there should be embankments, and sets of four ditches (see Table 3).

Table 3 Crop Growth in Plots With Different Forms and Spacings of Drains

(1)	(2)	(3)	(4)	3	4	5	6
(5) 播种 (月·日)	11.10	11.10	11.10	11.10	11.10	11.10	11.10
(6) 出苗 (月·日)	12.4	12.3	11.30	12.10	12.10	12.12	12.12
(7) 基本苗 (万/亩)	29.2	29.5	28.4	28.2	28.9	29.6	29.4
(8) 分蘖数 (万/亩)	55.2	51.0	46.9	42.2	42.2	46.9	46.9
(9) 拔节 (月·日)	3.15	3.15	3.15	3.15	3.15	3.15	3.15
(10) 抽穗 (月·日)	4.10	4.10	4.10	4.10	4.10	4.10	4.10
(11) 成熟 (月·日)	5.22	5.22	5.22	5.22	5.22	5.22	5.22
(12) 有效穗 (万/亩)	24.0	21.0	23.4	21.0	21.7	21.4	21.0
(13) 有效穗数	27.5	21.3	23.0	22.0	22.1	21.1	21.0
(14) 有效穗数	26.6	23.9	21.4	21.0	22.1	20.6	20.3
(15) 穗重 (g)	81.1	77.4	71.2	77.4	87.2	71.3	74.0
(16) 穗重 (g)	6.3	5.8	5.0	5.6	6.0	5.5	5.1
(17) 千粒重 (g)	38.1	38.5	36.8	37.7	38.0	36.7	36.7
(18) 实产 (斤/亩)	583.7	529.5	491.3	483.5	499.7	511.9	542.2

(1) item
(2) open drain
(3) open/underground drain
(4) underground drain
(5) sowing (month.day)
(6) budding (month.day)
(7) basic shoots (10,000 per mu)
(8) number of shoots during full tillering period
(9) jointing (month.day)
(10) earing (month.day)
(11) ripening (month.day)
(12) effective ears (10,000 per mu)
(13) total grains per ear
(14) number of full grains per ear
(15) plant height (cm)
(16) ear length (cm)
(17) weight of one thousand grains (gram)
(18) actual yield (jin per mu)

EARLY PLUM RAIN FORECASTING

Beijing QIXIANG [METEOROLOGY] in Chinese No 4, Apr 78 p 39

[Article in Special Section "Swapping Experiences Among Meteorological Posts" by Department of Geography, Red and Expert Normal School Fengxian County, Shanghai: "Long Range Forecasting of Early Plum Rain Period"]

[Text] Plum rain is closely related to summer harvesting and summer sowing. This is particularly true when plum rain sets in early and gravely affects summer harvesting and summer sowing. By combining Shanghai's 1949-1958 data and Fengxian's 1959-1977 data with actual local conditions, we have come up with the following periods at the advent of the plum rain season: early plum, which occurs from late May through early June; mid plum, in June; late plum, starting in late June; and empty plum, when there is no evident plum rain. The early, mid and late plums basically coincide with what are commonly known as grain bud golden plum [1420 3341 2734], golden plum [7806 2734] and rice-transplant plum [5335/2480/1407 2734].

Forecasting Early Plum Rain

Through data analysis, we have discovered that a certain relationship exists between early period temperature conditions and the early or late arrival of plum rain. Using the vertical axis for the sums of monthly mean temperatures

from October through December in the previous year ($\sum_{10}^{12} \bar{T}$), and the horizontal axis for the sums of monthly mean temperatures from January through April in the current year ($\sum_1^4 \bar{T}$), we composed the following point accumulation chart (Figure 1).



Figure 1

- (1) previous year
- (2) \circ early plum
- \square mid plum
- \diamond late plum
- \times empty plum

From Figure 1, it is evident that when $\sum_{10}^{12} \bar{T} \geq 35.7$ degrees Centigrade, the occurrence rate of early plum is 6/7 of the total number of times which early plum has occurred since 1949, with only the exception of 1954. Thus, in January of the current year, we can use $\sum_{10}^{12} \bar{T}$ to determine the probability of early plum throughout the current year.

In early May of the current year, the forecasting of early plum rain can be done by combining $\sum_{10}^{12} \bar{T}$ and $\sum_1^4 \bar{T}$. Indices are as follows:

1. If $\sum_{10}^{12} \bar{T} \geq 35.7$ degrees Centigrade, $\sum_1^4 \bar{T} \geq 30.1$ degrees Centigrade, and the mean temperature sums of March and April are within the range of 20.9 to 21.3 degrees Centigrade, then early plum rain will occur in the current year (4/4); on the other hand, if conditions are to the contrary, then mid plum rain or late plum rain will occur.

2. If $\sum_{10}^{12} \bar{T} \geq 35.7$ degrees Centigrade, $\sum_1^4 \bar{T} < 30.1$ degrees Centigrade, and the mean temperature of January in the current year is within the range of 7.2 to 7.5 degrees Centigrade, then early plum rain will occur in the current year (2/2); and, if conditions are to the contrary, mid plum or late plum rain will occur.

3. If $\sum_{10}^{12} \bar{T} < 35.7$ degrees Centigrade, $\sum_1^4 \bar{T} \geq 30.1$ degrees Centigrade, and the mean temperature sums of March and April are ≤ 20.2 degrees Centigrade, then early plum rain will occur in the current year; and, if conditions are to the contrary, mid or late plum rain will occur instead.

Forecasting Mid and Late Plum Rain

Through data analysis, we have also found out that the heaviest diurnal precipitation period is related to mid plum rain and late plum rain. Using the vertical axis for the maximum diurnal precipitation period in May, and the horizontal axis for the highest air temperature in May, we composed another point accumulation chart (Figure 2).

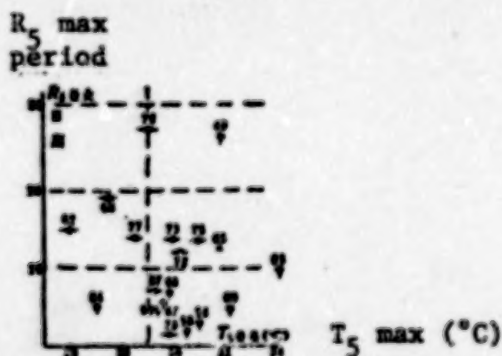


Figure 2

From Figure 2, it is evident that if the maximum diurnal precipitation comes in early May, then the late plum rain is most likely to occur (9/11); if the maximum diurnal precipitation comes in mid May, then mid plum (7/8) or empty plum (1/8) is bound to occur; if the maximum diurnal precipitation comes in late May, we will have to base our predictions with the help of the highest air temperature: If the highest air temperature in May exceeds 29 degrees Centigrade, it is late plum; and if ≤ 29 degrees Centigrade, then it is mid plum.

According to information recorded throughout the past 29 years, there was only one year (1965) of empty plum rain, and from Figure 1, it can be seen that the $\sqrt[4]{T}$ of that year was especially low, which may be used as reference for predicting empty plum rain in the future.

9119

CSO: 4008

AREAS OF INCLEMENT WEATHER CONDITIONS REPORTED

Beijing QIXIANG [METEOROLOGY] in Chinese No 4, Apr 78 p 39

[Article: "Information"]

[Text] According to statistics based on meteorological observation data since liberation, the most frequent hailfall area in China is located on the Qingzang [Tsinghai-Tibetan] Plateau, namely, Nagqu Region (4507.0 meters above sea level) in Xizang Province, where the average number of hailfall days each year is 34.5, and the maximum number of hail days per annum is 53.0. The most frequent frost-hit place is also found on the Qingzang Plateau, i.e., in Qinghai Province's Qingshui River; on the average, there are 245.6 frost days in a year, and the heaviest frost year is known to have reached 278.0 frost days. Sichuan Province's Mount Emei, which is situated 3047.4 meters above sea level, is the most frequent fog-hit area in the country—on the average, there are 323.4 days of fog annually, and the worst year is recorded to have 334.0 days of fog. The most frequent sandstorm area is located in Kalpin, Xinjiang Province (40°30' N, 79°03' E; 1161.8 meters above sea level); each year, the average number of sandstorm days is 38.5, and 53.0 days is the maximum ever recorded in a year. The place of most frequent thunderstorms is located in Mengla, which is found in Yunnan Province's Xishuangbanna region; thunderstorms average 128.3 days in a year, the maximum being 148.0 days. The most frequent snowfall area is Tianchi, Jilin Province (2670.0 meters above sea level), averaging 142.1 snowfall days per annum, and the maximum number of snow days in a year is 175.0. The most frequent and longest silver thaw places are found on Mount Emei; each year, silver thaw averages 135.2 days, and the maximum number of days ever recorded in a year is 167.0 days, the longest continuous period being, 3,198 hours 54 minutes.

9119

CSO: 4008

END

END OF

FICHE

DATE FILMED

Sept. 10, 1979
B.B.